

TABLE 3. Multivariate Cox regression analysis of recurrence-free survival according to various factors

Pathologic variables	All		Node negative		Node positive	
	HR	P value	HR	P value	HR	P value
LC ratio	0.44	.010	0.39	.008	1.7	.62
>30 vs <30	0.23-0.82		0.20-0.78		0.44-6.3	
Lymphatic invasion	2.5	.001	1.9	.045	6.1	.037
Positive vs negative	1.4-4.3		1.0-3.5		1.3-28.7	
Blood vessel invasion	1.8	.037	2.0	.031	0.87	.61
Positive vs negative	1.0-3.1		1.1-3.8		0.31-2.4	
Pleural invasion	1.6	.11	2.1	.024	0.47	.19
Positive vs negative	0.91-2.7		1.1-3.9		0.14-1.5	
Lymph node metastasis	1.9	.032	—*	—*	—*	—*
Positive vs negative	1.1-3.4					

LC, Lepidic component; HR, hazard ratio. *Not calculated.

micrometastatic disease to the lymph nodes have been demonstrated to have a worse prognosis than patients with lymph nodes completely replaced by tumors.¹⁵ This suggests that the continuum from LI to lymph node micrometastasis to lymph node replacement might be more complex than previously believed.

As in previous reports, in all patients, multivariate analysis of RFS revealed a lower LC ratio, positive status of lymph nodes, LI, blood vessel invasion, pleural invasion and were poor prognostic factors as well as N+ status in this study.^{16,17} In contrast, all evaluated pathologic variables, except for LI status, did not show potential as predictive factors for patients with lymph node involvement. Although lymphatic metastasis status was a strong prognostic factor, LI status was also a significant predictive factor of prognosis in patients with clinical stage IA lung adenocarcinoma. In pN+ patients, LI status had no association with either the clinical or pathologic findings. Thus, the above findings strongly support the significance of LI status as a predictive factor, particularly in patients whose lymph node status is clinically negative and pathologically positive. That is, poor prognosis should be defined according to not only lymph node status but also LI status. Other unknown factors may more precisely determine the true patient population with a poor prognosis. Although pN+ patients typically receive adjuvant chemotherapy, such patients may be classified into no-adjuvant, mild-adjuvant, and severe-adjuvant groups using several predictive factors, including LI status.

Two previous reports have demonstrated that LI status is a poor prognostic factor in surgically resected non-small cell lung cancer^{18,19} and a similar result was shown in pathologic stage I or adenocarcinoma patients. Additionally, LI status has been demonstrated to be a prognostic factor regardless of lymph node status.^{18,19} However, these previous studies had some limitations; 1 was the quality of LI status evaluation. LI status was evaluated using D2-40 immunostaining in this study,

whereas only some tumors were assessed for LI status using D2-40 in the report¹⁹ and the other did not distinguish LI from blood vessel invasion.¹⁸ Thus, the quality of LI evaluation was higher in our study. Another limitation is heterogeneity of the cohort. The analysis was performed only in pathologic stage I patients in the previous studies to minimize heterogeneity.^{18,19} However, that analysis of pathologic stage I patients could not assess LI status in pN+ patients. In our study, we evaluated LI status with little heterogeneity in pN+ patients because we included only clinical stage IA adenocarcinoma patients having little heterogeneity.

The rate of lymph node involvement was 6.7% of clinical stage IA lung adenocarcinoma patients in our study (41 out of 609 cases). PET/CT examination has been shown to provide the most accurate preoperative diagnosis^{1,4} and results in appropriate treatment. However, a new diagnostic method is necessary to evaluate more accurately the preoperative status of patients with clinical stage IA adenocarcinoma and pathologic lymph node involvement whose preoperative diagnostic modality included a PET scan.

Few patients had lymph node metastasis in clinical stage IA lung adenocarcinoma, which represents one of the main limitations of this study; only a very small number of patients with lymph node involvement had a negative LI status. This makes it difficult to conclude that the prognosis of pN(+)LI(-) patients is equivalent to that of pN(-)LI(+) patients; however, it cannot be denied that LI status plays an important role in assessing patients with lymph node metastasis. The lack of data about pathologic tumor size or morbidity are also limitations of our study. Another is that detailed numbers on patients who received postoperative chemotherapy were not available. Postoperative chemotherapy was performed when pathologic upstaging or recurrence was detected. Additionally, although the follow-up time was too short to assess OS in this study, the OS curves showed similar tendencies to RFS. Because a previous study reported that RFS could be a surrogate

TABLE 4. Clinicopathologic findings in patients with clinical stage IA but pathologic lymph node positive lung adenocarcinoma, according to lymphatic invasion status

Finding	Lymph node metastasis positive		P value
	Lymphatic invasion negative (n = 13)	Lymphatic invasion positive (n = 28)	
Age			
Median	64	66	.96
Interquartile range	56-72	55.25-73.25	
Sex			
Female	4	15	.20
Male	9	13	
CEA			
Median	3.7	3.4	.81
Interquartile range	2.5-4.075	2.65-4.25	
Size*			
Median	2	2.2	.62
Interquartile range	1.6-2.6	1.775-2.5	
GGO† ratio			
Median	0	0	.75
Interquartile range	0-10	0-2.5	
SUV max			
Median	3.4	3.7	.87
Interquartile range	2.7-4.0	2.175-4.925	
LC ratio			
Median	10	10	.16
Interquartile range	10-20	0-12.5	
Blood vessel invasion			
Negative	7	10	.32
Positive	6	18	
Pleural invasion			
Negative	11	18	.28
Positive	2	10	
Lymph node metastasis			
N1	9	11	.18
Single station N2 or single station N2 + N1	2	11	
Multistation N2	2	6	

CEA, Carcinoembryonic antigen; GGO, ground-glass opacity; SUV, standardized uptake value; LC, lepidic component. *Tumor size on the high-resolution computed tomography scan. †GGO ratio on the high-resolution computed tomography scan.

for OS,²⁰ to evaluate RFS may effectively be equivalent to assessing OS in identifying prognostic factors.

CONCLUSIONS

LI was not always present in pN+ adenocarcinoma patients. In addition, pN(+)/LI(-) patients had a better prognosis than pN(+)/LI(+) patients, whereas there was no significant difference in RFS between pN(+)/LI(-) and pN(-)/LI(+) patients with clinical stage IA lung adenocarcinoma. LI status was indicated to classify clinical T1 N0 M0 lung adenocarcinoma patients with and without lymph node involvement into good and poor prognosis groups, the preoperative staging of which conducted using high-resolution

CT and FDG-PET/CT. LI status may affect the selection of patients who have to receive adjuvant therapy.

References

- Lardinois D, Weder W, Hany TF, Kamel EM, Korom S, Seifert B, et al. Staging of non-small-cell lung cancer with integrated positron-emission tomography and computed tomography. *N Engl J Med*. 2003;348:2500-7.
- Okada M, Nakayama H, Okumura S, Daisaki H, Adachi S, Yoshimura M, et al. Multicenter analysis of high-resolution computed tomography and positron emission tomography/computed tomography findings to choose therapeutic strategies for clinical stage IA lung adenocarcinoma. *J Thorac Cardiovasc Surg*. 2011;141:1384-91.
- Tsutani Y, Miyata Y, Nakayama H, Okumura S, Adachi S, Yoshimura M, et al. Prediction of pathologic node-negative clinical stage IA lung adenocarcinoma for optimal candidates undergoing sublobar resection. *J Thorac Cardiovasc Surg*. 2012;144:1365-71.
- Shim SS, Lee KS, Kim BT, Chung MJ, Lee EJ, Han J, et al. Non-small cell lung cancer: prospective comparison of integrated FDG PET/CT and CT alone for preoperative staging. *Radiology*. 2005;236:1011-9.
- Kim BT, Lee KS, Shim SS, Choi JY, Kwon OJ, Kim H, et al. Stage T1 non-small cell lung cancer: preoperative mediastinal nodal staging with integrated FDG PET/CT—a prospective study. *Radiology*. 2006;241:501-9.
- Yi CA, Lee KS, Kim BT, Shim SS, Chung MJ, Sung YM, et al. Efficacy of helical dynamic CT versus integrated PET/CT for detection of mediastinal nodal metastasis in non-small cell lung cancer. *AJR Am J Roentgenol*. 2007;188:318-25.
- Lee SM, Park CM, Paeng JC, Im HJ, Goo JM, Lee HJ, et al. Accuracy and predictive features of FDG-PET/CT and CT for diagnosis of lymph node metastasis of T1 non-small-cell lung cancer manifesting as a subsolid nodule. *Eur Radiol*. 2012;22:1556-63.
- Goldstraw P, Crowley J, Chansky K, Giroux DJ, Groome PA, Rami-Porta R, et al. The IASLC Lung Cancer Staging Project: proposals for the revision of the TNM stage groupings in the forthcoming (seventh) edition of the TNM Classification of malignant tumours. *J Thorac Oncol*. 2007;2:706-14.
- Suzuki K, Koike T, Asakawa T, Kusumoto M, Asamura H, Nagai K, et al. A prospective radiological study of thin-section computed tomography to predict pathological noninvasiveness in peripheral clinical IA lung cancer (Japan Clinical Oncology Group 0201). *J Thorac Oncol*. 2011;6:751-6.
- Travis WD, Brambilla E, Muller-Hermelink HK, Harris CC. Pathology and genetics tumors of the lung, pleura, thymus and heart. In: World Health Organization classification of tumours. Lyon, France: IARC Press; 2004.
- Nakayama H, Okumura S, Daisaki H, Kato Y, Uehara H, Adachi S, et al. Value of integrated positron emission tomography revised using a phantom study to evaluate malignancy grade of lung adenocarcinoma: a multicenter study. *Cancer*. 2010;116:3170-7.
- Delbecq D, Coleman RE, Guiberteau MJ, Brown ML, Royal HD, Siegel BA, et al. Procedure guideline for tumor imaging with 18F-FDG PET/CT 1.0. *J Nucl Med*. 2006;47:885-95.
- Li L, Ren S, Zhang Y, Guan Y, Zhao J, Liu J, et al. Risk factors for predicting the occult nodal metastasis in T1-2N0M0 NSCLC patients staged by PET/CT: potential value in the clinic. *Lung Cancer*. 2013;81:213-7.
- Kanda Y. Investigation of the freely available easy-to-use software 'EZR' for medical statistics. *Bone Marrow Transplant*. 2013;48:452-8.
- Riquet M, Bagan P, Le Pimpee Barthes F, Banu E, Scotte F, Foucault C, et al. Completely resected non-small cell lung cancer: reconsidering prognostic value and significance of N2 metastases. *Ann Thorac Surg*. 2007;84:1818-24.
- Funai K, Sugimura H, Morita T, Shundo Y, Shimizu K, Shiiya N. Lymphatic vessel invasion is a significant prognostic indicator in stage IA lung adenocarcinoma. *Ann Surg Oncol*. 2011;18:2968-72.
- Kudo Y, Saji H, Shimada Y, Nomura M, Matsubayashi J, Nagao T, et al. Impact of visceral pleural invasion on the survival of patients with non-small cell lung cancer. *Lung Cancer*. 2012;78:153-60.
- Higgins KA, Chino JP, Ready N, D'Amico TA, Berry MF, Sporn T, et al. Lymphovascular invasion in non-small-cell lung cancer: implications for staging and adjuvant therapy. *J Thorac Oncol*. 2012;7:1141-7.
- Wang J, Wang B, Zhao W, Guo Y, Chen H, Chu H, et al. Clinical significance and role of lymphatic vessel invasion as a major prognostic implication in non-small cell lung cancer: a meta-analysis. *PLoS One*. 2012;7:e52704.
- Gill S, Sargent D. End points for adjuvant therapy trials: has the time come to accept disease-free survival as a surrogate end point for overall survival? *Oncologist*. 2006;11:624-9.

Involvement of homologous recombination in the synergism between cisplatin and poly (ADP-ribose) polymerase inhibition

Kenji Sakogawa,^{1,2} Yoshiro Aoki,^{1,2} Keizo Misumi,^{1,2} Yoichi Hamai,² Manabu Emi,² Jun Hihara,² Lin Shi,¹ Kazuteru Kono,¹ Yasunori Horikoshi,¹ Jiying Sun,¹ Tsuyoshi Ikura,³ Morihito Okada² and Satoshi Tashiro^{1,4}

Departments of ¹Cellular Biology, ²Surgical Oncology, Research Institute for Radiation Biology and Medicine, Hiroshima University, Hiroshima; ³Department of Mutagenesis, Radiation Biology Center, Kyoto University, Kyoto, Japan

(Received February 27, 2013/Revised July 31, 2013/Accepted August 29, 2013/Accepted manuscript online September 5, 2013/Article first published online October 10, 2013)

Poly (ADP-ribose) polymerase (PARP) plays a critical role in responding to DNA damage, by activating DNA repair pathways responsible for cellular survival. Inhibition of PARP is used to treat certain solid cancers, such as breast and ovarian cancers. However, its effectiveness with other solid cancers, such as esophageal squamous cell carcinoma (ESCC), has not been clarified. We evaluated the effects of PARP inhibition on the survival of human esophageal cancer cells, with a special focus on the induction and repair of DNA double-strand breaks. The effects were monitored by colony formation assays and DNA damage responses, with immunofluorescence staining of γ H2AX and RAD51. We found that PARP inhibition synergized with cisplatin, and the cells were highly sensitive, in a similar manner to the combination of cisplatin and 5-fluorouracil (5-FU). Comparable increases in RAD51 foci formation were observed after each combined treatment with cisplatin and either 3-aminobenzamide (3-AB) or 5-FU in three human esophageal cancer cell lines, TE11, TE14, and TE15. In addition, decreasing the amount of RAD51 by RNA interference rendered the TE11 cells even more hypersensitive to these treatments. Our findings suggested that the homologous recombinational repair pathway may be involved in the synergism between cisplatin and either 3-AB or 5-FU, and that 3-AB and 5-FU may similarly modify the cisplatin-induced DNA damage to types requiring the recruitment of RAD51 proteins for their repair. Understanding these mechanisms could be useful for improving the clinical outcome of ESCC patients who suffer from aggressive disease that presently lacks effective treatment options. (*Cancer Sci* 2013; 104: 1593–1599)

Genomic integrity is maintained by the close cooperation of several DNA repair pathways. Any failure in these pathways can lead to unrepaired DNA lesions, which cause cell-cycle arrest and cell death, either directly or following DNA replication during the S phase of the cell cycle.^(1,2) Therefore, the therapeutic effects of DNA-damaging agents may be enhanced by the inhibition of DNA repair. This feature makes DNA repair mechanisms a promising target for novel cancer treatment regimens.

In recent years, poly (ADP-ribose) polymerase (PARP) inhibitors have emerged as a novel class of chemotherapeutic agents. An abundant nuclear protein that catalyzes the formation of PAR polymers from NAD⁺, PARP is attached primarily to glutamic acid residues on acceptor proteins.⁽³⁾ It participates in maintaining genomic integrity, as it is a DNA damage-sensing protein that binds to DNA single-strand breaks (SSBs).^(4,5) In addition, PARP plays a role in restarting stalled replication forks, by attracting Mre11 to these sites.^(6,7) Therefore, the inhibition of PARP generates DNA damage, and the obstructed

replication forks can be converted to replication-associated DNA double-strand breaks (DSBs), which lead to cell cycle arrest and cell death unless they are repaired by the homologous recombinational repair pathway (HR).^(8,9) Recently, the PARP inhibitors in clinical use have been shown to trap the PARP1 and PARP2 enzymes at damaged DNA.⁽¹⁰⁾ The trapped PARP–DNA complexes are more cytotoxic than the unrepaired SSBs caused by PARP inactivation, as the complexes require other genetic repair pathways, such as postreplication repair and the Fanconi anemia pathway, in addition to HR, for their repair.⁽¹⁰⁾

Double-strand breaks are potentially lethal, and are generally considered to be the most toxic DNA lesions.^(11,12) Direct DSBs are mainly repaired by the non-homologous end joining pathway,⁽¹³⁾ whereas replication-associated DSBs are repaired by the HR and related replication repair pathways.⁽⁹⁾ The HR and PARP are intricately linked, because the loss of PARP results in an increase in the recombinogenic lesions normally repaired by HR.^(14–17) Therefore, tumor cells defective in HR show extremely high sensitivity to PARP inhibitors.^(18–24) In addition, it was recently reported that PARP inhibition sensitizes even HR-proficient tumor cells to ionizing radiation or alkylating agents, such as methyl methanesulfonate, when treated in combination for a short time.⁽²⁵⁾

Esophageal squamous cell carcinoma (ESCC) is one of the most lethal malignant diseases, especially in the USA and Europe.^(26,27) Based on biochemical modulation studies,^(28,29) combined therapy with cisplatin and 5-fluorouracil (5-FU) has recently shown encouraging results, by exerting a synergistic cytotoxic effect. However, the clinical outcomes and the overall survival rates of ESCC patients remain poor.⁽³⁰⁾ The present study was carried out to evaluate the effects of PARP inhibition on the cellular survival and the DNA damage response in human esophageal cancer cells, with a special focus on DSB induction and repair. We found that PARP inhibition synergized with cisplatin, and strongly increased the percentage of cells bearing nuclear foci of RAD51, a key protein in the HR pathway. This combined therapy was as efficient as the combined treatment with cisplatin and 5-FU, as compared to that with each drug alone. Importantly, RAD51 depletion significantly sensitized the cells to these combined treatments. Our data suggested that HR may be involved in the synergism between cisplatin and either a PARP inhibitor or 5-FU in human esophageal cancer cells. In addition, the PARP inhibitor and 5-FU may similarly modify the cisplatin-induced DNA damage to types requiring the recruitment of RAD51 proteins for their repair.

⁴To whom correspondence should be addressed.
E-mail: ktashiro@hiroshima-u.ac.jp

Materials and Methods

Cells and chemicals. Three human esophageal cancer cell lines, TE11, TE14, and TE15, were obtained from the Cell Resource Center for the Biomedical Research Institute of Development, Aging, and Cancer (Tohoku University, Sendai, Japan). Both TE11 and TE14 are moderately differentiated squamous cell carcinomas, and TE15 is a well-differentiated squamous cell carcinoma. These cell lines were routinely grown in RPMI-1640 (Invitrogen, Carlsbad, CA, USA) supplemented with 10% FBS, and incubated at 37°C in a humidified atmosphere of 5% CO₂ in air. The PARP inhibitor 3-aminobenzamide (3-AB) was obtained from Sigma-Aldrich (#A0788; St. Louis, MO, USA). Cisplatin (Nippon Kayaku, Tokyo, Japan) and 5-FU (Kyowa Hakko Kogyo, Tokyo, Japan) were dissolved in PBS at 1 mM.

Detailed experimental procedures are also provided in the supplementary experimental procedures (Data S1).

Results

Inhibition of PARP in ESCC cell lines. To examine whether PARP inhibition could be efficacious in the treatment of ESCC, we first tested three ESCC cell lines, TE11, TE14, and TE15, for their sensitivity to PARP inhibition. We confirmed the inactivation of PARP by a PARP inhibitor, 3-AB, and the depletion of PARP1 by siRNAs, using immunoblotting analyses (Figs S1, S2A), and then measured the cell viability by a colony formation assay. This assay showed that 3-AB did not decrease the viability of these ESCC cells, as compared to the untreated controls (Fig. 1a).

As PARP inhibition increases the collapse of unresolved SSBs into DSBs at replication forks,^(31,32) we investigated the induction of DSBs by PARP inhibition in these ESCC cells. Thus, we carried out immunofluorescence staining for γ H2AX, as a marker of DSBs, after the treatment of the ESCC cell lines with 3-AB. As a result, mild increases in the percentages of γ H2AX foci-positive cells were observed in all of these cells after the 3-AB treatment (Figs 1b–d, S3A). As the inhibition of PARP by 3-AB treatment did not impair the colony

forming activity, most of the DSBs generated by the PARP inhibition might be exactly repaired, and thus not induce cell cycle arrest or cell death. This notion was supported by similar findings obtained by experiments using PARP1-depleted cells in place of 3-AB treatment (Fig. S2A,B).

Combination of PARP inhibition with cisplatin or 5-FU in ESCC cell lines. Cisplatin and 5-FU are effective chemotherapeutic agents used with ESCC patients.^(28,29) We wished to examine whether PARP inhibition acts synergistically with either cisplatin or 5-FU against esophageal cancer cells. Thus, we treated TE11, TE14, and TE15 cells with either cisplatin or 5-FU, with or without the inhibition of PARP, and then carried out a colony formation assay to assess the cellular survival after these treatments (Fig. S4). The colony assay revealed that 3-AB sensitized all of these cell lines to cisplatin (Fig. 2a). The synergistic inhibition of cell growth was observed by the combined treatment of TE11 cells with 5 μ M cisplatin and 5 mM 3-AB (Fig. S5, Combination Index = 0.471). In stark contrast, no synergism between 3-AB and 5-FU was observed (Fig. 2a).

To explore the reason for this distinct sensitization of cells to cisplatin and 5-FU by 3-AB, we next studied the levels of γ H2AX focus formation generated by each treatment. The combined treatment with cisplatin and 3-AB induced significantly higher percentages of γ H2AX focus formation compared to the single treatment with cisplatin (Figs 2b,c, S3A). The γ H2AX focus formation of TE11 cells peaked at 24 h, and 60% of cells remained foci-positive even at 48 h after treatment (Fig. 2d). Combined treatment with 5-FU and 3-AB induced γ H2AX focus formation with similar increases and kinetics as the single treatment with 5-FU, and it peaked at 24 h after treatment (Figs 2b,c,e, S3A). Although the TE15 cells treated with 5-FU and 3-AB showed a lower percentage of γ H2AX foci-positive cells, as compared to the 5-FU single treatment, the average numbers of γ H2AX foci per cell generated by these treatments were similar to those of the other cell lines (Figs 2b, S3A). Similar findings were obtained by the depletion of PARP1 using siRNA, instead of 3-AB treatment (Fig. S2C). Therefore, the significantly increased induction of DSBs by PARP inhibition could

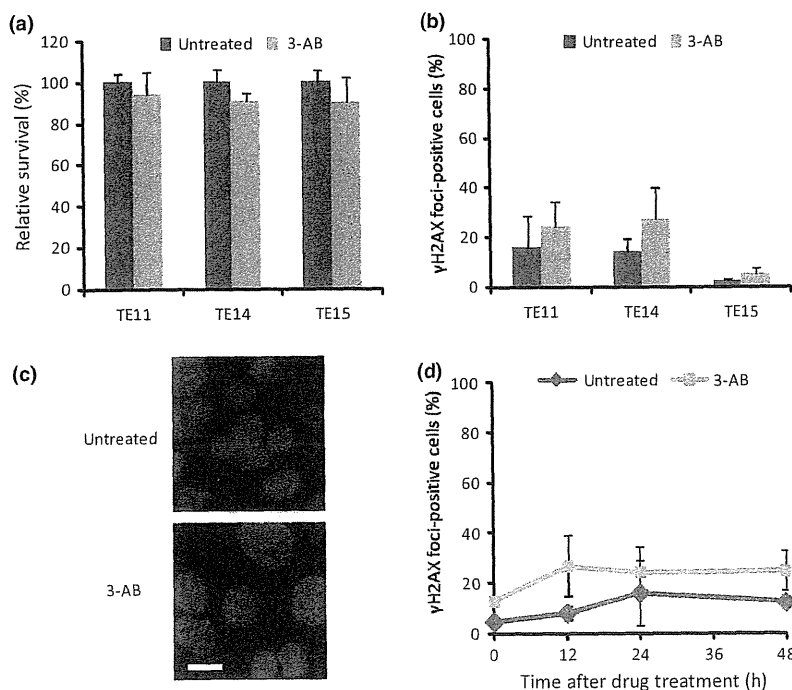


Fig. 1. Poly (ADP-ribose) polymerase (PARP) inhibition by 3-aminobenzamide (3-AB) in human esophageal cancer cell lines. (a) Survival of TE11, TE14, and TE15 cells after treatment with 3-AB. (b) Induction of double-strand breaks, indicating γ H2AX focus formation, at 24 h after PARP inhibition by 3-AB in TE11, TE14, and TE15 cells. (c) DNA (blue) and γ H2AX foci (red) were visualized at 24 h after treatment of TE11 cells. Scale bar = 10 μ m. (d) Kinetics of γ H2AX foci formation at the indicated periods up to 48 h, after 3-AB pretreatment for 48 h. Cells with 10 or more foci were counted as positive. At least 200 nuclei were counted for each experiment. The average and SD from at least three experiments are shown.

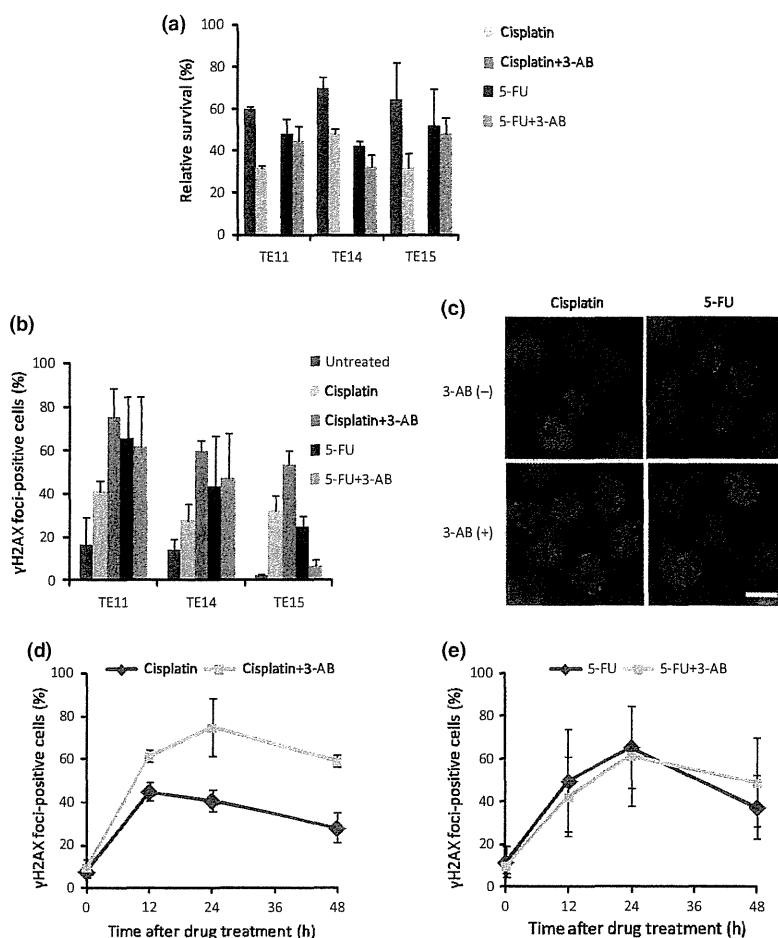


Fig. 2. Combination of a poly (ADP-ribose) polymerase (PARP) inhibitor 3-aminobenzamide (3-AB) with cisplatin or 5-fluorouracil (5-FU) in human esophageal cancer cell lines. (a) Survival of TE11, TE14, and TE15 cells after treatment with either 5 μ M cisplatin for 1 h or 3 μ M 5-FU for 24 h, with or without pretreatment with 3 mM (TE14) or 5 mM (TE11 and TE15) 3-AB for 48 h. (b) Evaluation of the γ H2AX focus formation at 24 h after treatment of TE11, TE14, and TE15 cells with either cisplatin or 5-FU, with or without pretreatment with 3-AB. (c) DNA (blue) and γ H2AX foci (red) were visualized at 24 h after treatment of TE11 cells. Scale bar = 10 μ m. (d,e) TE11 cells were treated with either cisplatin or 5-FU, with or without pretreatment with 3-AB. Cells with 10 or more foci were counted as positive. At least 200 nuclei were counted for each experiment. The average and SD from at least three experiments are shown.

enhance the cytotoxic effects of cisplatin treatment of these ESCC cells.

Modulation of ESCC cell sensitivity to combined treatment with cisplatin and 5-FU by PARP inhibition. Having established that the PARP inhibitor could sensitize ESCC cells to cisplatin, we next compared the anticancer effects between the combined treatments with cisplatin/3-AB and cisplatin/5-FU, the most standard chemotherapy for ESCC. We treated the ESCC cells with cisplatin and 5-FU in concurrent combinations, and then measured the cell viability by a colony formation assay. As a result, all of the ESCC cell lines treated with cisplatin plus 5-FU showed similar high degrees of sensitivity to the cisplatin plus PARP inhibition (Figs 2a,3a,S2B).

To clarify the reason for the high sensitivity of the ESCC cells to the combined treatment with cisplatin and 5-FU, we next carried out an immunofluorescence assay for γ H2AX proteins in these cell lines. This assay revealed that the γ H2AX focus formation following the cisplatin plus 5-FU treatment was quite consistent with that following the cisplatin plus 3-AB treatment (Figs 2b,d,3b,d,S3A). Thus, we hypothesized that 3-AB and 5-FU might play analogous roles in the increased numbers of DSBs formed in combination with cisplatin, resulting in the similar sensitivities of the cells to combined treatments with cisplatin and either 3-AB or 5-FU.

To confirm our hypothesis, we next investigated the cytotoxic effect of the triple combination of 3-AB, cisplatin, and 5-FU against ESCC cells. First, we inhibited PARP by 3-AB or depleted it by siRNAs, and then treated the cells concurrently with cisplatin and 5-FU. The cellular survival was confirmed by a colony formation assay. This assay

showed that the triple treatment did not cause a further decrease in the survival of the cells, as compared to the combined treatment with cisplatin and either 3-AB or 5-FU (Figs 2a,3a).

Next, we examined the γ H2AX focus formation, to assess the induction of DSBs by the triple treatment of the ESCC cells. Immunofluorescence staining analysis of γ H2AX revealed that the level of γ H2AX focus formation induced by the triple treatment was not significantly different from that induced by the combined treatment with cisplatin and either 3-AB or 5-FU in these cells (Figs 2b–d,3b–d,S3A). Similar findings were obtained by PARP1 depletion instead of 3-AB treatment (Fig. S2B,C). Therefore, these findings indirectly supported our hypothesis that PARP inhibition and 5-FU increase the sensitivity of ESCC cells to cisplatin, by disturbing the same pathway involving the induction or repair of DNA damage.

Validation of HR, indicating RAD51 foci formation in ESCC cells. Poly (ADP-ribose) polymerase inhibition induces DSBs, which require HR for their repair.^(31,32) Thus, we next examined the involvement of HR after the induction of DSBs by PARP inhibition, to understand the mechanisms underlying the synergism between cisplatin and either 3-AB or 5-FU in ESCC cells. We assessed RAD51 focus formation, as a hallmark of ongoing HR, after treatments with 3-AB, cisplatin, and 5-FU alone and in combination.

Immunofluorescence staining of RAD51 revealed that the 3-AB treatment significantly increased the percentage of cells with RAD51 foci, as compared to the untreated controls (Figs 4a–c,S3B). As 3-AB did not disturb the colony formation

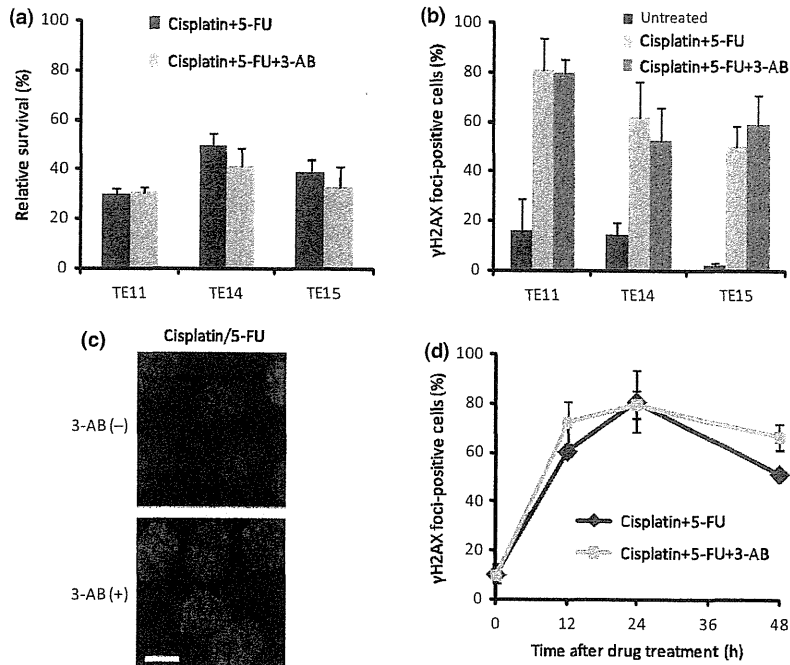


Fig. 3. Comparison of standard combined treatments for esophageal squamous cell carcinoma using cisplatin and 5-fluorouracil (5-FU) with or without poly (ADP-ribose) polymerase (PARP) inhibition. (a) Survival of TE11, TE14, and TE15 cells after concurrent combined treatments with cisplatin and 5-FU, with or without pretreatment with 3-aminobenzamide (3-AB). (b) Evaluation of the γ H2AX focus formation at 24 h after combined treatment of TE11, TE14, and TE15 cells with cisplatin and 5-FU, with or without a pretreatment with 3-AB. (c) DNA (blue) and γ H2AX foci (red) were visualized at 24 h after treatment of TE11 cells. Scale bar = 10 μ m. (d) TE11 cells were treated with cisplatin and 5-FU in concurrent combination, after pretreatment with 3-AB. Cells with 10 or more foci were counted as positive. At least 200 nuclei were counted for each experiment. The average and SD from at least three experiments are shown.

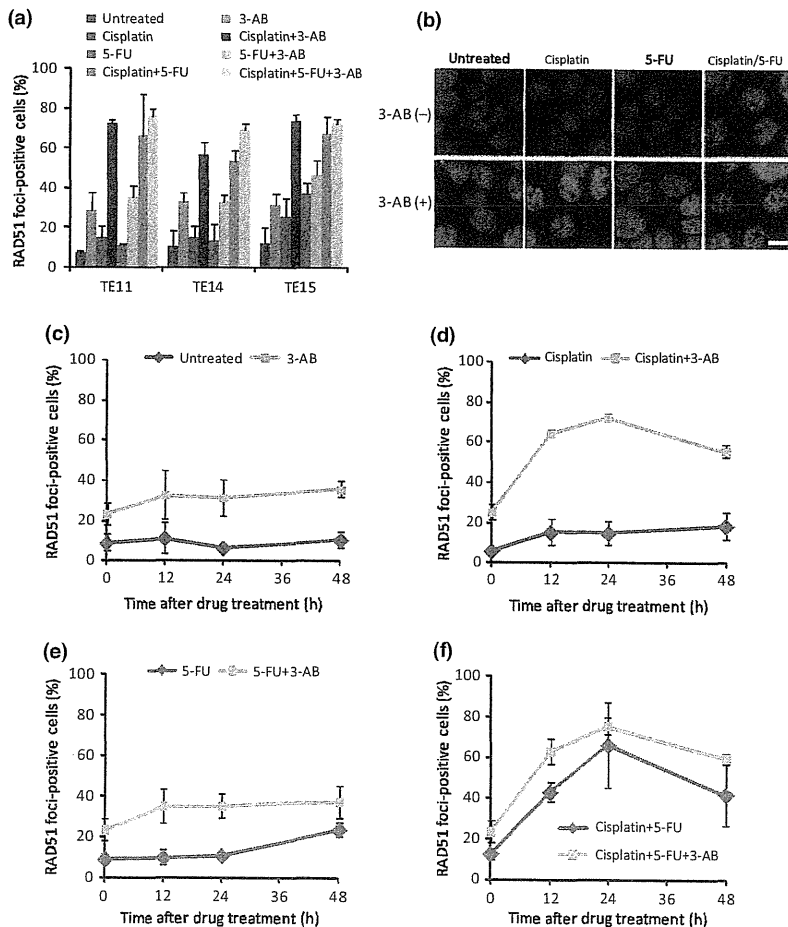


Fig. 4. Validation of the homologous recombination repair pathway in esophageal squamous cell carcinoma cells, indicating RAD51 focus formation. (a) Evaluation of the RAD51 focus formation 24 h after treatment of TE11, TE14, and TE15 cells with cisplatin or 5-fluorouracil (5-FU) alone and in combination, with or without a pretreatment with 3-aminobenzamide (3-AB). (b) Representative images of DNA (blue) and RAD51 foci (green) 24 h after the treatment of TE11 cells. Scale bar = 10 μ m. (c) TE11 cells were treated with or without 3-AB. (d,e) TE11 cells were treated with either cisplatin or 5-FU, with or without pretreatment with 3-AB. (f) TE11 cells were treated concurrently with cisplatin and 5-FU, after pretreatment with 5 mM 3-AB for 48 h. Cells with five or more foci were counted as positive. At least 200 nuclei were counted for each experiment. The average and SD from three experiments are shown.

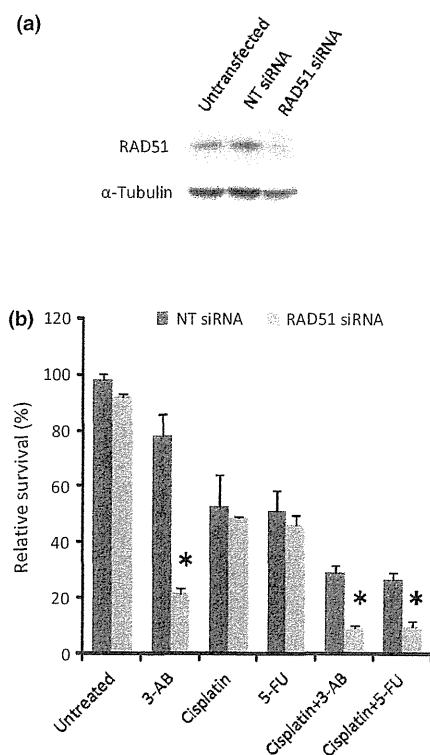


Fig. 5. Knockdown of RAD51 protein renders esophageal squamous cell carcinoma TE11 cells hypersensitive to combinations of cisplatin and either 3-aminobenzamide (3-AB) or 5-fluorouracil (5-FU). (a) Immunoblotting analysis of RAD51 (top) and α -tubulin (bottom) in TE11 cells, after RAD51 siRNA or non-targeting (NT) siRNA depletion for 24 h. (b) Relative survival of TE11 cells treated with 3-AB, cisplatin, and 5-FU alone and in combination, under the same experimental conditions after RAD51 siRNA or NT siRNA depletion for 24 h, confirmed by colony formation assay. The average and SD from at least three experiments are shown. Values marked with asterisks are statistically significant, as compared with each control ($*P < 0.05$).

activity of the ESCC cells (Fig. 1a), this finding suggested that the 3-AB-induced DNA damage might be exactly repaired by HR.

The treatment of cells with cisplatin or 5-FU alone caused only a slight increase in the percentage of RAD51 foci-positive cells up to 48 h after treatment. However, the combined treatment of these cells with cisplatin and either 3-AB or 5-FU markedly increased the percentage of cells with RAD51 foci, which reached a maximum at 24 h after each treatment (Figs 4,S3B). When used in combination with cisplatin, both 3-AB and 5-FU vigorously promoted the production of DSBs, which require the recruitment of RAD51 proteins for their repair in these ESCC cells.

The PARP-inhibited ESCC cells treated with or without 5-FU showed similar levels of RAD51 focus formation after each treatment (Figs 4a–c,e,S3B). Moreover, the addition of 5-FU did not change the kinetics of RAD51 focus formation by the combined treatment with cisplatin and 3-AB (Figs 4a,b,d,f,S3B). These data suggested that 5-FU might not affect the RAD51 focus formation induced by 3-AB, with or without cisplatin, in these ESCC cells. Similar results were obtained by the depletion of PARP1 in place of 3-AB treatment (Fig. S2D). Thus, the validation of HR additionally supported our hypothesis that the enhancement of the anticancer effect of cisplatin, by either PARP inhibition or 5-FU, might be attributed to similar mechanisms involving HR repair in ESCC cells.

Depletion of RAD51 enhances 3-AB- or 5-FU-mediated sensitization of ESCC cells to cisplatin. As RAD51 plays crucial and well-established roles in HR,^(33–35) we hypothesized that the critical role of HR would be the underlying reason for the synergistic effect of cisplatin and either 3-AB or 5-FU in ESCC cells. Thus, we examined how RAD51 depletion affected the sensitivity of TE11 cells to these combined treatments. The depletion of RAD51 by siRNAs was confirmed by an immunoblotting analysis, using anti-RAD51 antibodies (Figs 5a,S6A).

We treated RAD51-knockdown cells with either 3-AB, cisplatin, and 5-FU alone or in combination, under the same experimental conditions as described above, and then the cellular survival was measured by a colony formation assay (Figs 5b,S6B). As expected, RAD51 depletion caused a drastic increase in the cellular sensitivity to 3-AB. In contrast, RAD51 knockdown showed neither a synergistic nor an additive effect on the sensitivity to cisplatin or 5-FU alone (Figs 5b,S6B). These findings suggested that HR might play a major role in the repair of DNA damage induced by treatment with 3-AB, but not with cisplatin or 5-FU alone. In contrast to the treatment with cisplatin or 5-FU alone, RAD51 repression significantly sensitized the TE11 cells to cisplatin in combination with either 3-AB or 5-FU. Considering our finding that the addition of 3-AB to treatment with 5-FU or cisplatin/5-FU did not enhance the γ H2AX focus formation (Figs 2b,e,3b,d,S3A), these data supported our hypothesis that the conversion of cisplatin-induced DNA damage to the types requiring HR for their repair could play an important role in TE11 cells sensitization to cisplatin by both 3-AB and 5-FU.

Discussion

Our data showed that the inhibition of PARP exerts a synergistic tumor-cell killing effect in combination with cisplatin, but not 5-FU, against three ESCC cell lines, TE11, TE14, and TE15, by the increased induction of DNA damage requiring HR for repair. Moreover, in the sensitization of cells to cisplatin, PARP inhibition by 3-AB and 5-FU may function by similar mechanisms involving HR.

Poly (ADP-ribose) polymerase inhibitors were originally developed to selectively target HR-defective cells, and have been tested as a monotherapy and in combination with an alkylating agent and cisplatin in patients with certain solid tumors.^(36–39) In this study, 3-AB, as a single agent, had minimal cytotoxic efficacy (Fig. 1a), and only modest increases of γ H2AX and RAD51 focus formation in response to 3-AB were observed in the ESCC cells, as compared to the untreated controls (Figs 1b,4a). These data indicated that the DSBs induced by 3-AB may be exactly repaired by HR, and therefore, these cells are predicted to be proficient in HR repair.⁽⁴⁰⁾ Thus, consistent with a previous study,⁽²⁵⁾ PARP inhibitors, in combination with certain DNA damaging agents, could be useful in the treatment of even HR-proficient cancer cells.

Poly (ADP-ribose) polymerase and RAD51 are required to reactivate replication at stalled DNA forks.^(6,7,41,42) Therefore, the synergism between cisplatin and either 3-AB or 5-FU may be similarly attributed to the failure of replication reactivation at stalled replication forks, due to the inhibition of PARP activity or the incorporation of 5-FU into replicating DNA in the cisplatin-induced DNA lesions. This failure may lead to increased RAD51 focus formation, for the efficient restarting of stalled replication forks by HR. The addition of 3-AB to either the 5-FU or cisplatin/5-FU treatment neither facilitated nor repressed the cellular survival and γ H2AX/RAD51 focus formation (Figs 2a,b,3a,b,4a), therefore, 3-AB and 5-FU may function in an epistatic pathway for the cisplatin-induced DNA lesion repair in ESCC cells. Our results suggested that a novel regimen, combining cisplatin with a PARP inhibitor, may have

similar efficacy to the standard combined chemotherapy of cisplatin and 5-FU in the treatment of ESCC patients.

In conclusion, we have shown that HR may be involved in the synergism between cisplatin and either PARP inhibition or 5-FU treatment, in human esophageal cancer cell lines. Our findings provide a platform for extending the potential use of PARP inhibitors to ESCC patients. Poly (ADP-ribose) polymerase inhibitors could be novel combinational counterparts of cisplatin in the treatment of ESCC. Moreover, cancer cells with decreased RAD51 activity, due to mutations or dysregulation, would be more sensitive to PARP inhibitors than the surrounding HR-proficient tissue.^(43,44) Therefore, considering the therapeutic potential of PARP inhibitors in the treatment of ESCC, such cases would be ideal candidates for PARP inhibitor therapy, and the side-effects usually seen with classical cytotoxic anticancer drugs could be minimized.

Although it may be premature to extrapolate our results from only three cultured cell lines, further investigations of the mechanisms responsible for the increases of RAD51 foci, in combination with cisplatin and either PARP inhibition or 5-FU treatment, in human cancer cells will provide novel insights into cancer therapies.

Acknowledgment

This work was supported by the Grants-in-Aid Program from the Ministry of Education, Culture, Sports, Science and Technology of Japan.

Disclosure Statement

The authors have no conflict of interest.

References

- 1 Hoijmakers JH. Genome maintenance mechanisms for preventing cancer. *Nature* 2001; **411**: 366–74.
- 2 Farmer H, McCabe N, Lord CJ *et al*. Targeting the DNA repair defect in BRCA mutant cells as a therapeutic strategy. *Nature* 2005; **434**: 917–21.
- 3 Satoh MS, Lindahl T. Role of poly (ADP-ribose) formation in DNA repair. *Nature* 1992; **356**: 356–8.
- 4 Lindahl T, Satoh MS, Poirier GG, Klungland A. Post-translational modification of poly (ADP-ribose) polymerase induced by DNA strand breaks. *Trends Biochem Sci* 1995; **20**: 405–11.
- 5 D'Amours D, Desnoyers S, D'Silva I, Poirier GG. Poly(ADP-ribose)ylation reactions in the regulation of nuclear functions. *Biochem J* 1999; **342**: 249–68.
- 6 Bryant HE, Petermann E, Schultz N *et al*. PARP is activated at stalled forks to mediate Mre11-dependent replication restart and recombination. *EMBO J* 2009; **28**: 2601–15.
- 7 Yang YG, Cortes U, Patnaik S, Jasin M, Wang ZQ. Ablation of PARP-1 does not interfere with the repair of DNA double-strand breaks, but compromises the reactivation of stalled replication forks. *Oncogene* 2004; **23**: 3872–82.
- 8 Schultz N, Lopez E, Saleh-Gohari N, Helleday T. Poly (ADP-ribose) polymerase (PARP-1) has a controlling role in homologous recombination. *Nucleic Acids Res* 2003; **31**: 4959–64.
- 9 Arnaudeau C, Lundin C, Helleday T. DNA double-strand breaks associated with replication forks are predominantly repaired by homologous recombination involving an exchange mechanism in mammalian cells. *J Mol Biol* 2001; **307**: 1235–45.
- 10 Murai J, Huang SY, Das BB *et al*. Trapping of PARP1 and PARP2 by clinical PARP inhibitors. *Cancer Res* 2012; **72**: 5588–99.
- 11 Hsiang YH, Lihou MG, Liu LF. Arrest of replication forks by drug-stabilized topoisomerase I-DNA cleavable complexes as a mechanism of cell killing by camptothecin. *Cancer Res* 1989; **49**: 5077–82.
- 12 Markovits J, Pommier Y, Kerrigan D, Covey JM, Tilchen EJ, Kohn KW. Topoisomerase II-mediated DNA breaks and cytotoxicity in relation to cell proliferation and the cell cycle in NIH 3T3 fibroblasts and L1210 leukemia cells. *Cancer Res* 1987; **47**: 2050–5.
- 13 Sargent RG, Brenneman MA, Wilson JH. Repair of site-specific double-strand breaks in a mammalian chromosome by homologous and illegitimate recombination. *Mol Cell Biol* 1997; **17**: 267–77.
- 14 Magnusson J, Ramel C. Inhibitor of poly (ADP-ribose)transferase potentiates the recombinogenic but not the mutagenic action of alkylating agents in somatic cells in vivo in *Drosophila melanogaster*. *Mutagenesis* 1990; **5**: 511–4.
- 15 Waldman AS, Waldman BC. Stimulation of intrachromosomal homologous recombination in mammalian cells by an inhibitor of poly(ADP-ribose)ylation. *Nucleic Acids Res* 1991; **19**: 5943–7.
- 16 Schreiber V, Hunting D, Trucco C *et al*. A dominant-negative mutant of human poly (ADP-ribose) polymerase affects cell recovery, apoptosis and sister chromatid exchange following DNA damage. *Proc Natl Acad Sci USA* 1995; **92**: 4753–7.
- 17 Semionov A, Courmoyer D, Chow TY. Inhibition of poly (ADP-ribose)polymerase stimulates extrachromosomal homologous recombination in mouse Ltk-fibroblasts. *Nucleic Acids Res* 1999; **27**: 4526–31.
- 18 Donawho CK, Luo Y, Luo Y *et al*. ABT-888, an orally active poly (ADP-ribose) polymerase inhibitor that potentiates DNA-damaging agents in preclinical tumor models. *Clin Cancer Res* 2007; **13**: 2728–37.
- 19 Penning TD, Zhu GD, Gandhi VB *et al*. Discovery of the Poly (ADP-ribose) polymerase (PARP) inhibitor 2-[(R)-2-methylpyrrolidin-2-yl]-1H-benzimidazole-4-carboxamide (ABT-888) for the treatment of cancer. *J Med Chem* 2009; **52**: 514–23.
- 20 Evers B, Drost R, Schut E *et al*. Selective inhibition of BRCA2-deficient mammary tumor cell growth by AZD2281 and cisplatin. *Clin Cancer Res* 2008; **14**: 3916–25.
- 21 Hay T, Matthews JR, Pietzka L *et al*. Poly (ADP-ribose) polymerase-1 inhibitor treatment regresses autochthonous Brca2/p53-mutant mammary tumors in vivo and delays tumor relapse in combination with carboplatin. *Cancer Res* 2009; **69**: 3850–5.
- 22 Menear KA, Adcock C, Boulter R *et al*. 4-[3-(4-cyclopropanecarbonylpiperazine-1-carbonyl)-4-fluorobenzyl]-2H-phthalazin-1-one: a novel bioavailable inhibitor of poly (ADP-ribose) polymerase-1. *J Med Chem* 2008; **51**: 6581–91.
- 23 Rottenberg S, Jaspers JE, Kersbergen A *et al*. High sensitivity of BRCA1-deficient mammary tumors to the PARP inhibitor AZD2281 alone and in combination with platinum drugs. *Proc Natl Acad Sci USA* 2008; **105**: 17079–84.
- 24 Jones P, Altamura S, Boueres J *et al*. Discovery of 2-{4-[(3S)-piperidin-3-yl]phenyl}-2H-indazole-7-carboxamide (MK-4827): a novel oral poly (ADP-ribose)polymerase (PARP) inhibitor efficacious in BRCA-1 and -2 mutant tumors. *J Med Chem* 2009; **52**: 7170–85.
- 25 Löser DA, Shibata A, Shibata AK, Woodbine LJ, Jeggo PA, Chalmers AJ. Sensitization to radiation and alkylating agents by inhibitors of poly (ADP-ribose) polymerase is enhanced in cells deficient in DNA double-strand break repair. *Mol Cancer Ther* 2010; **9**: 1775–87.
- 26 Parkin DM, Bray F, Ferlay J, Pisani P. Global cancer statistics, 2002. *CA Cancer J Clin* 2005; **55**: 74–108.
- 27 Shimada H, Nabeya Y, Okazumi S *et al*. Prediction of survival with squamous cell carcinoma antigen in patients with resectable esophageal squamous cell carcinoma. *Surgery* 2003; **133**: 486–94.
- 28 Sekiguchi H, Akiyama S, Fujiwara M *et al*. Phase II trial of 5-fluorouracil and low-dose cisplatin in patients with squamous cell carcinoma of the esophagus. *Surg Today* 1999; **29**: 97–101.
- 29 Scanlon KJ, Newman EM, Lu Y, Priest DG. Biochemical basis for cisplatin and 5-fluorouracil synergism in human ovarian carcinoma cells. *Proc Natl Acad Sci USA* 1986; **83**: 8923–5.
- 30 Borghesi S, Hawkins MA, Tait D. Oesophagectomy after definitive chemoradiation in patients with locally advanced oesophageal cancer. *Clin Oncol (R Coll Radiol)* 2008; **20**: 221–6.
- 31 Bryant HE, Schultz N, Thomas HD *et al*. Specific killing of BRCA2-deficient tumours with inhibitors of poly (ADP-ribose) polymerase. *Nature* 2005; **434**: 913–7.
- 32 Saleh-Gohari N, Bryant HE, Schultz N, Parker KM, Cassel TN, Helleday T. Spontaneous homologous recombination is induced by collapsed replication forks that are caused by endogenous DNA single-strand breaks. *Mol Cell Biol* 2005; **25**: 7158–69.
- 33 Lim DS, Hasty P. A mutation in mouse rad51 results in an early embryonic lethal that is suppressed by a mutation in p53. *Mol Cell Biol* 1996; **16**: 7133–43.
- 34 Tsuzuki T, Fujii Y, Sakumi K *et al*. Targeted disruption of the Rad51 gene leads to lethality in embryonic mice. *Proc Natl Acad Sci USA* 1996; **93**: 6236–40.
- 35 Sonoda E, Sasaki MS, Buerstedde JM *et al*. Rad51-deficient vertebrate cells accumulate chromosomal breaks prior to cell death. *EMBO J* 1998; **17**: 598–608.

- 36 Turner N, Tutt A, Ashworth A. Hallmarks of "BRCAness" in sporadic cancers. *Nat Rev Cancer* 2004; **4**: 814–9.
- 37 Vesprini D, Narod SA, Trachtenberg J *et al*. The therapeutic ratio is preserved for radiotherapy or cisplatin treatment in BRCA2-mutated prostate cancers. *Can Urol Assoc J* 2011; **5**: E31–5.
- 38 Plummer R, Jones C, Middleton M *et al*. Phase I study of the poly (ADP-ribose) polymerase inhibitor, AG014699, in combination with temozolomide in patients with advanced solid tumors. *Clin Cancer Res* 2008; **14**: 7917–23.
- 39 Rajan A, Carter CA, Kelly RJ *et al*. A phase I combination study of olaparib with cisplatin and gemcitabine in adults with solid tumors. *Clin Cancer Res* 2012; **18**: 2344–51.
- 40 Mukhopadhyay A, Elattar A, Cerbinskaite A *et al*. Development of a functional assay for homologous recombination status in primary cultures of epithelial ovarian tumor and correlation with sensitivity to poly (ADP-ribose) polymerase inhibitors. *Clin Cancer Res* 2010; **16**: 2344–51.
- 41 Davies SL, North PS, Hickson ID. Role for BLM in replication-fork restart and suppression of origin firing after replicative stress. *Nat Struct Mol* 2007; **14**: 677–9.
- 42 Petermann E, Orta ML, Issaeva N, Schultz N, Helleday T. Hydroxyurea-stalled replication forks become progressively inactivated and require two different RAD51-mediated pathways for restart and repair. *Mol Cell* 2010; **37**: 492–502.
- 43 Rouleau M, Patel A, Hendzel MJ, Kaufmann SH, Poirier GG. PARP inhibition: PARP1 and beyond. *Nat Rev Cancer* 2010; **10**: 293–301.
- 44 Ashworth A. A synthetic lethal therapeutic approach: poly(ADP) ribose polymerase inhibitors for the treatment of cancers deficient in DNA double-strand break repair. *J Clin Oncol* 2008; **26**: 3785–90.

Supporting Information

Additional supporting information may be found in the online version of this article:

Fig. S1. Immunoblotting analysis of poly (ADP-ribose) PAR and poly (ADP-ribose) polymerase 1 (PARP1) in esophageal squamous cell carcinoma TE11 cells after exposure to 3-aminobenzamide (3-AB).

Fig. S2. Treatment of poly (ADP-ribose) polymerase 1 (PARP1)-depleted esophageal squamous cell carcinoma TE11 cells with anticancer drugs.

Fig. S3. Numbers of γ H2AX and RAD51 foci per nucleus after treatment with anticancer drugs.

Fig. S4. Time schedule of treatments with anticancer drugs.

Fig. S5. Dose–response analysis of the survival of esophageal squamous cell carcinoma TE11 cells treated with cisplatin and 3-aminobenzamide (3-AB) in combination.

Fig. S6. Knockdown of RAD51 protein using RAD51 siRNA (#2) also renders TE11 cells hypersensitive to combinations of cisplatin and either 3-aminobenzamide (3-AB) or 5-fluorouracil (5-FU).

Data S1. Supplementary experimental procedures and discussion.

Oncologic outcomes of segmentectomy compared with lobectomy for clinical stage IA lung adenocarcinoma: Propensity score–matched analysis in a multicenter study

Yasuhiro Tsutani, MD, PhD,^a Yoshihiro Miyata, MD, PhD,^a Haruhiko Nakayama, MD, PhD,^b Sakae Okumura, MD, PhD,^c Shuji Adachi, MD, PhD,^d Masahiro Yoshimura, MD, PhD,^e and Morihito Okada, MD, PhD^a

Objective: Our objective was to compare the oncologic outcomes of lobectomy and segmentectomy for clinical stage IA lung adenocarcinoma.

Methods: We examined 481 of 618 consecutive patients with clinical stage IA lung adenocarcinoma who underwent lobectomy or segmentectomy after preoperative high-resolution computed tomography and F-18-fluorodeoxyglucose positron emission tomography/computed tomography. Patients (n = 137) who underwent wedge resection were excluded. Lobectomy (n = 383) and segmentectomy (n = 98) as well as surgical results were analyzed for all patients and their propensity score–matched pairs.

Results: Recurrence-free survival (RFS) and overall survival (OS) were not significantly different between patients undergoing lobectomy (3-year RFS, 87.3%; 3-year OS, 94.1%) and segmentectomy (3-year RFS, 91.4%; hazard ratio [HR], 0.57; 95% confidence interval [CI], 0.27-1.20; *P* = .14; 3-year OS, 96.9%; HR, 0.49; 95% CI, 0.17-1.38; *P* = .18). Significant differences in clinical factors such as solid tumor size (*P* < .001), maximum standardized uptake value (SUVmax) (*P* < .001), and tumor location (side, *P* = .005; lobe, *P* = .001) were observed between both treatment groups. In 81 propensity score–matched pairs including variables such as age, gender, solid tumor size, SUVmax, side, and lobe, RFS and OS were similar between patients undergoing lobectomy (3-year RFS, 92.9%, 3-year OS, 93.2%) and segmentectomy (3-year RFS, 90.9%; 3-year OS, 95.7%).

Conclusions: Segmentectomy is suitable for clinical stage IA lung adenocarcinoma, with survivals equivalent to those of standard lobectomy. (*J Thorac Cardiovasc Surg* 2013;146:358-64)

Segmentectomy for treating small lung cancer has been a topic of debate for a long time. In 1995, the Lung Cancer Study Group conducted a prospective randomized controlled trial comparing limited resection (including segmentectomy and wedge resection) with lobectomy for clinical T1 N0 M0 non–small cell lung cancer (NSCLC). The study concluded that limited resection resulted in higher local recurrence and lower survival.¹ A recent study from the Surveillance Epidemiology and End Results database showed that lobectomy conferred a significant advantage compared with segmentectomy in stage I NSCLC.² In contrast, several studies reported that the survivals after segmentectomy and

those after lobectomy were similar.³⁻⁷ However, few reports compare between segmentectomy and lobectomy with matched patient variables affecting survival.

Recently, we^{8,9} reported that solid tumor size, defined as the maximum dimension of the solid component excluding the ground-glass opacity (GGO) component on high-resolution computed tomography (HRCT), and maximum standardized uptake value (SUVmax) on [18F]-fluoro-2-deoxy-D-glucose positron emission tomography/computed tomography (FDG-PET/CT), are useful for predicting the pathologic invasiveness or prognosis in clinical stage IA lung adenocarcinoma. These preoperative radiologic findings are important when choosing treatment strategies for NSCLC, particularly for lung adenocarcinoma.^{8,9}

The purpose of this retrospective study was to compare the oncologic outcomes between lobectomy and segmentectomy in patients with clinical stage IA lung adenocarcinoma, adjusted for preoperative factors including HRCT and FDG-PET/CT findings, to minimize the effect of patient selection bias. Segmentectomy and wedge resection are considerably different procedures for lung cancer; the former can be used to approach hilar lymph nodes and to get sufficient margin, whereas the latter cannot. Therefore, we excluded wedge resection from this study.

From the Department of Surgical Oncology,^a Hiroshima University, Hiroshima; the Department of Thoracic Surgery,^b Kanagawa Cancer Center, Yokohama; the Department of Thoracic Surgery,^c Cancer Institute Hospital, Tokyo; and the Departments of Radiology^d and Thoracic Surgery,^e Hyogo Cancer Center, Akashi, Japan.

Disclosures: Authors have nothing to disclose with regard to commercial support. Received for publication Oct 4, 2012; revisions received Jan 10, 2013; accepted for publication Feb 11, 2013; available ahead of print March 13, 2013.

Address for reprints: Morihito Okada, MD, PhD, Department of Surgical Oncology, Research Institute for Radiation Biology and Medicine, Hiroshima University, 1-2-3-Kasumi, Minami-ku, Hiroshima City, Hiroshima 734-0037, Japan (E-mail: morihito@hiroshima-u.ac.jp).

0022-5223/\$36.00

Copyright © 2013 by The American Association for Thoracic Surgery
http://dx.doi.org/10.1016/j.jtcvs.2013.02.008

Abbreviations and Acronyms

CI	= confidence interval
FDG-PET/CT	= [18F]-fluoro-2-deoxy-D-glucose positron emission tomography/computed tomography
GGO	= ground-glass opacity
HRCT	= high-resolution computed tomography
NSCLC	= non-small cell lung cancer
OS	= overall survival
RFS	= recurrence-free survival
SUVmax	= maximum standardized uptake value

PATIENTS AND METHODS**Patients**

We enrolled 618 patients with clinical T1 N0 M0 stage IA lung adenocarcinoma from 4 institutions (Hiroshima University, Kanagawa Cancer Center, Cancer Institute Hospital, and Hyogo Cancer Center, Japan) between August 1, 2005 and June 30, 2010, to evaluate the significance of FDG-PET/CT. Patients with incompletely resected tumors (R1 or R2) and those with multiple tumors or previous lung operations were not included in the database. The database has been maintained prospectively. The patient data obtained from this multicenter database were retrospectively analyzed in the present study. HRCT and FDG-PET/CT followed by curative R0 resection were performed for all patients staged according to the TNM Classification of Malignant Tumors, seventh edition.¹⁰ Mediastinoscopy or endobronchial ultrasonography was not routinely performed because all patients received preoperative HRCT and FDG-PET/CT; HRCT revealed no swelling of mediastinal or hilar lymph nodes and FDG-PET showed no accumulation in these lymph nodes. Sublobar resection was allowed in cases of complete removal of the disease, using the optional procedure instead of lobectomy for a peripheral T1 N0 M0 tumor. The other patients underwent standard lobectomy. All patients who underwent segmentectomy were suitable for lobectomy and all patients who underwent lobectomy were technically suitable for segmentectomy. Patients who had lymph node metastasis pathologically received platinum-based chemotherapy after operation.

The inclusion criteria were preoperative staging determined by HRCT and FDG-PET/CT, curative surgery without neoadjuvant chemotherapy or radiotherapy, and a definitive histopathologic diagnosis of lung adenocarcinoma. The study was approved by the institutional review boards of the participating institutions; the requirement for informed consent from individual patients was waived because the study was a retrospective review of the patient database. Of the 618 patients, 137 who underwent wedge resection were excluded; the remaining 481 were included in this analysis.

HRCT

Sixteen-row multidetector CT was used to obtain chest images independent of subsequent FDG-PET/CT examinations. For high-resolution images of the tumors, the following parameters were used: 120 kVp, 200 mA, 1- to 2-mm section thickness, 512 × 512-pixel resolution, 0.5- to 1.0-second scanning time, a high-spatial reconstruction algorithm with a 20-cm field of view, and mediastinal (level, 40 HU; width, 400 HU) and lung (level, -600 HU; width, 1600 HU) window settings. GGO was defined as a misty increase in lung attenuation without obscuring the

underlying vascular markings. We defined solid tumor size as the maximum dimension of the solid component measured on lung window settings, excluding GGO.⁸ CT scans were reviewed and tumor sizes were determined by radiologists from each institution.

FDG-PET/CT

Patients were instructed to fast for at least 4 hours before intravenous injection of 74 to 370 MBq FDG and were then advised to rest for at least 1 hour before FDG-PET/CT scanning. Blood glucose levels were calculated before the tracer injection to confirm a level of more than 150 mg/dL.¹¹ Patients with blood glucose levels of 150 mg/dL or more were excluded from the PET/CT imaging. For imaging, Discovery ST (GE Healthcare, Little Chalfont, United Kingdom), Aquiduo (Toshiba Medical Systems Corporation, Tochigi, Japan), or Biograph Sensation 16 (Siemens Healthcare, Erlangen, Germany) integrated 3-dimensional PET/CT scanner was used. Low-dose nonenhanced CT images of 2- to 4-mm section thickness for attenuation correction and localization of lesions identified by PET were obtained from the head to the pelvic floor of each patient according to a standard protocol.

Immediately after CT, PET was performed with the identical axial field of view for 2- to 4-min/table position, depending on the condition of the patient and the scanner performance. An iterative algorithm with CT-derived attenuation correction was used to reconstruct all PET images with a 50-cm field of view. An anthropomorphic body phantom (NEMA NU2-2001, Data Spectrum Corp, Hillsborough, NC) was used to minimize the variations in SUVs among the institutions.¹² A calibration factor was analyzed by dividing the actual SUV by the gauged mean SUV in the phantom background to decrease interinstitutional SUV inconsistencies; the final SUV used in this study is referred to as the revised SUVmax.^{13,14} When the SUVmax ratio was expressed as the SUVmax of each institute relative to the SUVmax of the control institute, the adjustment of interinstitutional variations in SUV narrowed the range from 0.89-1.24 to 0.97-1.18. The original SUVmax values were determined by radiologists from each institution.

Follow-up Evaluation

All patients who underwent lung resection were followed up from the day of surgery. Postoperative follow-up procedures, including a physical examination and chest radiograph every 3 months and chest and abdominal CT examinations every 6 months, were performed for the first 2 years. Subsequently, a physical examination and chest radiograph were performed every 6 months, and a chest CT examination was performed every year.

Statistical Analysis

Data are presented as numbers (percent) or the median unless otherwise stated. The χ^2 test for categorical variables was used to compare frequencies, and Fisher's exact test was applied to small samples in all cohorts. McNemar tests were used to analyze the propensity-matched pair patients. Both *t* tests and Mann-Whitney *U* tests were used to compare continuous variables in all cohorts. Wilcoxon tests were used to analyze propensity-matched pair patients. Recurrence-free survival (RFS) was defined as the time from the day of surgery until the first event (relapse or death from any cause) or last follow-up. Overall survival (OS) was defined as the time from the day of surgery until death from any cause or the last follow-up. The Kaplan-Meier method was used to analyze the duration of RFS and OS; the Cox proportional hazard model was used to assess differences in RFS and OS. We applied propensity score matching to balance the assignment of the included patients and to correct for the operative procedure (lobectomy or segmentectomy), which confounded survival calculations. The variables were age, gender, solid tumor size, SUVmax, side, and lobe. Because no segmentectomy was performed for a tumor located at a middle lobe, we excluded patients who underwent middle lobectomy from the scoring for a fair comparison. Each variable was multiplied by

TABLE 1. Patient characteristics

	Lobectomy (n = 383)	Segmentectomy (n = 98)	P value
Age	66 (33-84)	67 (34-89)	.08
Gender			.75
Male	169 (44.1%)	45 (45.9%)	
Whole tumor size (cm)	2.2 (0.8-3.0)	1.7 (0.6-3.0)	<.001
Solid tumor size (cm)	1.5 (0-3.0)	0.5 (0-3.0)	<.001
SUVmax	2.1 (0-17)	1.2 (0-10)	<.001
Side			.005
Right	261 (68.4%)	52 (53.1%)	
Lobe			.001
Upper	200 (52.2%)	50 (51.0%)	
Middle	45 (11.7%)	0 (0%)	
Lower	138 (36.0%)	48 (49.0%)	
Lymphatic invasion	77 (20.1%)	6 (6.1%)	.001
Vascular invasion	89 (23.2%)	6 (6.1%)	<.001
Pleural invasion	51 (13.3%)	4 (4.1%)	.008
Lymph node metastasis	44 (11.5%)	1 (1.0%)	<.001

SUVmax, Maximum standardized uptake value.

a coefficient that was calculated using logistic regression analysis, and the sum of these values was taken as the propensity score for individual patients. C statistic of variables was 0.819 (95% confidence interval [CI], 0.776-0.863; $P < .0001$). After the calculation of their propensity scores, the subjects were divided into 3 groups according to tertile to compare characteristics between lobectomy and segmentectomy in each tertile. For matching, lobectomy and segmentectomy pairs with an equivalent propensity score were selected by a 1-to-1 match. Statistical Package for the Social Sciences (SPSS) software (version 10.5; SPSS Inc, Chicago, Ill) was used to statistically analyze the data.

RESULTS

Table 1 summarizes the characteristics of the 481 patients analyzed in this study. Of these, 383 patients underwent lobectomy and 98 patients underwent segmentectomy. There was no 30-day postoperative mortality in this population. The median follow-up period after surgery was 43.2 months, during which the tumor recurred in 50 patients. There were 20 local-only recurrences, including mediastinal lymph node metastasis, and 30 distant \pm local recurrences. Age and gender were not significantly different between patients who underwent lobectomy and those who underwent segmentectomy. Lobectomy was performed significantly more often for patients with large whole and solid tumor size, high SUVmax, pathologically invasive tumors (presence of lymphatic, vascular, or pleural invasion), and lymph node involvement. Tumor location was significantly different between patients who underwent lobectomy and those who underwent segmentectomy. Detailed procedures in segmentectomy were shown in Table 2.

Local recurrence occurred in 17 patients who underwent lobectomy (2 involving the bronchial stump, 1 involving the hilar lymph nodes, 11 involving the mediastinal lymph nodes, and 3 involving the pleura) and 3 patients who

TABLE 2. Details of segmentectomy (n = 98)

Site	No.	Site	No.
Right		Left	
S1	4	S1 + 2	7
S2	12	S3	3
S3	3	S1 + 2 + 3	10
S6	23	S1 + 2 + 3c	1
S8	5	S4	2
S7 + 8	1	S5	1
S8 + 9	3	S4 + 5	7
S7 + 8 + 9 + 10	1	S6	10
		S8	1
		S9	3
		S6 + 8 + 9 + 10	1

underwent segmentectomy (1 involving the residual lobe, 1 involving the surgical stump, and 1 involving the pleura).

Table 3 shows the multivariate analyses of distant and local RFS. Gender, solid tumor size, and SUVmax were significant independent prognostic factor for distant RFS, whereas whole tumor size was not. Regarding local RFS, solid tumor size and SUVmax were independent prognostic factors, but whole tumor size was not. RFS was not significantly different between patients who underwent lobectomy (3-year RFS, 87.3%) compared with segmentectomy (3-year RFS, 91.4%; hazard ratio [HR], 0.57; 95% CI, 0.27-1.20; $P = .14$, Figure 1, A). OS was not significantly different between patients who underwent lobectomy (3-year OS, 94.1%) compared with segmentectomy (3-year OS, 96.9%; HR, 0.49; 95% CI, 0.17-1.38; $P = .18$; Figure 1, B).

After the calculation of the propensity score, the subjects were divided into 3 groups according to tertile (Table 4). The numbers of patients in tertiles 1, 2, and 3 according to the operative procedures (lobectomy; segmentectomy) were 79 and 66, 118 and 27, and 141 and 5, respectively. Solid tumor size was smaller and SUVmax was lower in the lowest tertile group, indicating that segmentectomy trended to be performed in patients with a tumor of smaller solid tumor size and lower SUVmax. There were some differences in background characteristics, especially in the lowest tertile group. Therefore, we performed propensity score matching to compare the survival between lobectomy and segmentectomy groups.

When propensity score matching was used and variables such as age, gender, solid tumor size, SUVmax, side, and lobe were included, lobectomy and segmentectomy pairs were well matched (81 patients each) without significant differences in clinical and pathologic factors (Table 5).

Among propensity score-matched patients, no difference in RFS was identified between patients who underwent lobectomy (3-year RFS, 92.9%) compared with segmentectomy (3-year RFS, 90.9%; Figure 1, C). In addition, similar OSs were observed between patients who underwent

TABLE 3. Multivariate analyses for distant or local RFS

Variables	HR (95% CI)	P value
Multivariate analysis for distant RFS		
Model 1		
Age	1.00 (0.96-1.04)	.86
Gender		
Male vs female	2.62 (1.15-5.95)	.022
Whole tumor size (cm)	1.17 (0.60-2.27)	.65
SUVmax	1.26 (1.14-1.39)	<.001
Procedure		
Lobectomy vs segmentectomy	1.44 (0.41-5.00)	.57
Model 2		
Age	1.00 (0.96-1.03)	.80
Gender		
Male vs female	2.57 (1.14-5.78)	.023
Solid tumor size (cm)	1.86 (1.09-3.16)	.023
SUVmax	1.19 (1.06-1.34)	.003
Procedure		
Lobectomy vs segmentectomy	0.90 (0.24-3.36)	.88
Multivariate analysis for local RFS		
Model 1		
Age	1.04 (0.99-1.10)	.15
Gender		
Male vs female	0.59 (0.24-1.46)	.26
Whole tumor size (cm)	1.44 (0.66-3.12)	.94
SUVmax	1.17 (1.03-1.33)	.015
Procedure		
Lobectomy vs segmentectomy	1.06 (0.29-3.86)	.36
Model 2		
Age	1.04 (0.98-1.09)	.19
Gender		
Male vs female	0.58 (0.24-1.43)	.24
Solid tumor size (cm)	2.89 (1.52-5.50)	.001
SUVmax	1.09 (0.94-1.27)	.26
Procedure		
Lobectomy vs segmentectomy	0.54 (0.14-2.13)	.38

RFS, Recurrence-free survival; HR, hazard ratio; CI, confidence interval; SUVmax, maximum standardized uptake value.

lobectomy (3-year OS, 93.2%) compared with segmentectomy (3-year OS, 95.7%; Figure 1, D).

DISCUSSION

The current study compared oncologic outcomes between patients who underwent lobectomy and segmentectomy for clinical stage IA lung adenocarcinoma. In all cohorts, when preoperative clinical factors were not adjusted, RFS and OS of the segmentectomy group were not significantly different from those of the lobectomy group. The survival curves of the segmentectomy group appeared to be better than those of the lobectomy group. However, each patient group was different in terms of solid tumor size and SUVmax, which could affect the patient's survival.^{8,9,13-16} In addition, the number of patients who had lymph node metastasis was inevitably larger in the lobectomy group

than in the segmentectomy group, which also could affect the survival. To minimize patient selection bias, we used propensity score matching analyses. In the model that matched for potentially confounding variables such as age, gender, solid tumor size, SUVmax, tumor location, in lobectomy and segmentectomy pairs, there were no significant differences in clinical features or pathologic factors such as lymphatic, vascular, pleural invasion, or lymph node metastasis. Even in our matched model, RFS and OS in the segmentectomy group was similar to the lobectomy group, indicating that segmentectomy could be an optimal surgical procedure for clinical stage IA lung adenocarcinoma selected on the basis of HRCT and FDG-PET/CT.

The strength of this study was that variables such as findings from HRCT (solid tumor size) and FDG-PET (SUVmax) were included in the propensity score-matched analysis. We reported that solid tumor size on HRCT and SUVmax on FDG-PET/CT had higher predictive values with respect to pathologic invasiveness such as lymphatic, vascular, pleural invasion, and prognosis compared with whole tumor size.^{8,9} In addition, once matching for solid tumor size and SUVmax, pure solid tumor and solid tumor with GGO showed equivalent survivals.¹⁷ Indeed, whole tumor size was not an independent factor for distant or local RFS in this study, whereas solid tumor size and SUVmax were. Solid tumor size does represent tumor malignancy compared with whole tumor size. Therefore, we did not include whole tumor size in matching variables. Inasmuch as SUVmax on FDG-PET/CT was a prognostic indicator for lung adenocarcinoma, not for squamous cell carcinoma in our previous study,¹⁶ the database included only adenocarcinoma, which is a major histologic type for NSCLC. Although several studies have indicated equivalent survivals for segmentectomy and lobectomy in patients with clinical stage IA lung cancer, to our knowledge, this is the first study adjusting for preoperative HRCT and FDG-PET/CT findings, both of which should be considered when selecting patients for limited resections such as segmentectomy. Furthermore, we used an anthropomorphic body phantom to minimize the interinstitutional variability in SUV, which may be influenced by factors such as preparation procedures, scan acquisition, image reconstruction, and data analysis.

Most previous studies that showed favorable outcomes with segmentectomy indicated this procedure for T1 N0 M0 NSCLC of 2 cm or less.⁴⁻⁶ We included patients with a whole tumor size of 2 to 3 cm (ie, clinical T1b tumor) in this study. We⁹ have reported that patients with T1b lung adenocarcinomas selected on the basis of HRCT and FDG-PET/CT findings could be candidates for sublobar resection with a sufficient surgical margin. Inasmuch as clinical T1b N0 M0 lung adenocarcinomas occasionally show large GGO components and/or low SUVmax (signs of

GTS

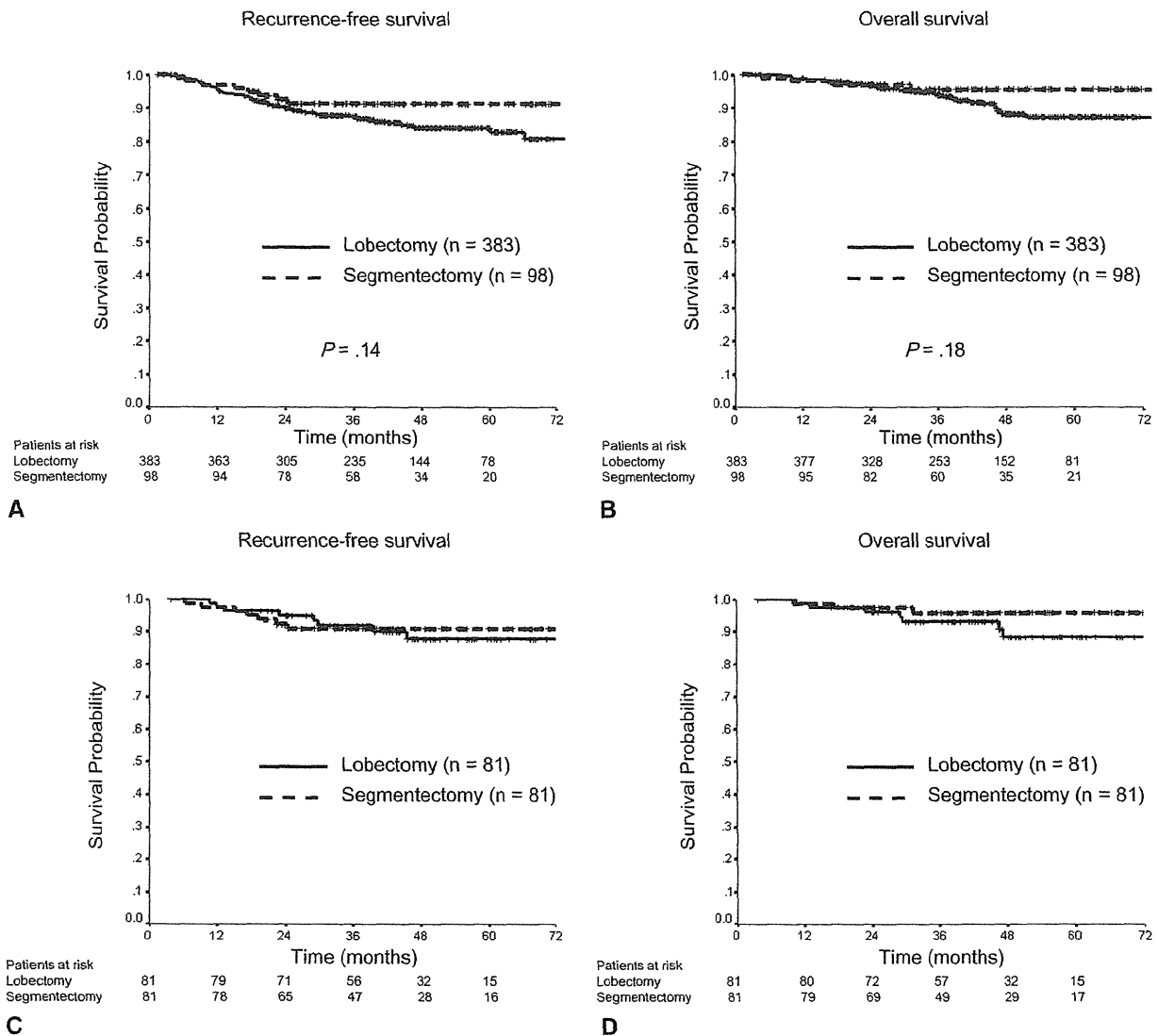


FIGURE 1. Recurrence-free survival (RFS) curves and overall survival (OS) curves for patients who underwent lobectomy and segmentectomy. A, In all cohorts, 3-year RFSs of 87.3% (mean RFS, 66.8 months; 95% confidence interval [CI], 64.6-69.4 months) and 91.4% (mean RFS, 70.3 months; 95% CI, 66.9-73.8 months) were identified for patients who underwent lobectomy and segmentectomy, respectively (hazard ratio [HR], 0.57; 95% CI, 0.27-1.20; $P = .14$). B, In all cohorts, 3-year OSs of 94.1% (mean OS, 70.4 months; 95% CI, 68.7-72.1 months) and 96.9% (mean OS, 72.9 months; 95% CI, 70.3-75.4 months) were identified for patients who underwent lobectomy and segmentectomy, respectively (HR, 0.49; 95% CI, 0.17-1.38; $P = .18$). C, In propensity score-matched patients, 3-year RFSs of 92.9% (mean RFS, 68.6 months; 95% CI, 64.9-72.2 months) and 90.9% (mean RFS, 70.2 months; 95% CI, 66.4-73.9 months) were identified for patients who underwent lobectomy and segmentectomy, respectively. D, In propensity score-matched patients, 3-year OSs of 93.2% (mean OS, 69.3 months; 95% CI, 65.8-72.7 months) and 95.7% (mean OS, 73.2 months; 95% CI, 70.6-75.8 months) were identified for patients who underwent lobectomy and segmentectomy, respectively.

low malignant behavior), such tumors could be treated with lesser resection.⁹

This study has several limitations. Because this study was retrospective, patients who underwent segmentectomy were possibly highly selective. In addition, we could not match intended procedures in the study because the database included only performed surgical procedures, not intended procedures, and patients with R1 or R2 resection were never included in the database. Most patients who underwent

segmentectomy in this study tended to have relatively low-malignancy tumors, with small solid tumor size and/or low SUVmax, and thus low pathologic invasiveness. The present study revealed that large solid tumor size on HRCT and high SUVmax on FDG-PET/CT were significantly associated with both local and distant recurrences. The outcome of segmentectomy for relatively high-malignancy clinical stage IA lung adenocarcinomas with large solid tumor size and high SUVmax is unclear.

TABLE 4. Patient characteristics divided into 3 groups according to tertile based on the propensity score

	Tertile 1			Tertile 2			Tertile 3		
	L (n = 79)	S (n = 66)	P value	L (n = 118)	S (n = 27)	P value	L (n = 141)	S (n = 5)	P value
Age	68 (48-82)	68.5 (42-89)	.53	65 (40-83)	65 (34-86)	.92	65 (33-84)	64 (53-83)	.5
Gender			.87			.28			1.0
Male	36 (45.6%)	29 (43.9%)		46 (39.0%)	14 (51.9%)		65 (46.1%)	2 (40.0%)	
Whole tumor size (cm)	2.0 (0.8-3.0)	1.7 (0.9-3.0)	.01	1.8 (1.0-3.0)	1.6 (0.6-2.9)	.048	2.5 (1.2-3.0)	2.4 (1.5-3.0)	.51
Solid tumor size (cm)	0.5 (0-2.0)	0.3 (0-1.0)	.056	1.4 (0-2.0)	1.2 (0-2.0)	.03	2.3 (1.0-3.0)	2.2 (1.0-3.0)	.71
SUVmax	1.2 (0-4.9)	1.0 (0-4.1)	.002	1.9 (0.6-8.3)	1.9 (0.4-9.8)	.77	3.9 (0.7-16.9)	2.1 (1.5-4.3)	.13
Side			.41			1.0			1.0
Right	44 (55.7%)	32 (48.5%)		69 (58.5%)	16 (59.3%)		103 (73.0%)	4 (80.0%)	
Lobe			.51			.53			1.0
Upper	41 (51.9%)	30 (45.5%)		66 (55.9%)	17 (63.0%)		93 (66.0%)	3 (60.0%)	
Lower	38 (48.1%)	36 (54.5%)		52 (44.1%)	10 (37.0%)		48 (34.0%)	2 (40.0%)	

L, Lobectomy; S, segmentectomy; SUVmax, maximum standardized uptake value.

Although surgical procedure did not correlate with local or distant recurrence in this study, segmentectomy for such tumors (ie, with large solid tumor size or high SUVmax) should be carefully considered. A clinical trial is being conducted by the Japanese Clinical Oncology Group/West Japan Oncology Group (JCOG0802/WJOG4607L), which aims to compare the surgical results between lobectomy and segmentectomy for T1 N0 M0 NSCLC measuring 2 cm or less.¹⁸ This prospective study includes patients with radiologically invasive tumors, such as solid dominant tumors, that have large solid tumor size on HRCT. The results of this trial may provide an important insight into this issue.

Segmentectomy is beneficial because it preserves lung function. Although the database used in this study did not incorporate lung function data, several reports have

demonstrated that segmentectomy has functional advantages over lobectomy.^{5,19,20} If similar oncologic outcomes are expected, segmentectomy should be considered for patients with clinical stage IA lung adenocarcinoma.

In conclusion, the oncologic outcomes of segmentectomy are similar to those of standard lobectomy for patients with clinical stage IA lung adenocarcinoma, as determined by the matched model adjusting for preoperative clinical factors such as HRCT and FDG-PET/CT findings. Segmentectomy could be favorable for selective patients with stage IA lung adenocarcinoma.

References

- Ginsberg RH, Rubinstein LV. Randomized trial of lobectomy versus limited resection for T1N0 non-small cell lung cancer. Lung Cancer Study Group. *Ann Thorac Surg.* 1995;60:615-23.
- Whitson BA, Groth SS, Andrade RS, Maddaus MA, Habermann EB, D'Cunha J. Survival after lobectomy versus segmentectomy for stage I non-small cell lung cancer: a population-based analysis. *Ann Thorac Surg.* 2011;92:1943-50.
- Jensik RJ, Faber LP, Milloy FJ, Monson DO. Segmental resection for lung carcinoma: a fifteen-year experience. *J Thorac Cardiovasc Surg.* 1973;66:563-72.
- Okada M, Yoshikawa K, Hata T, Tsubota N. Is segmentectomy with lymph node assessment an alternative to lobectomy for non-small cell lung cancer of 2 cm or smaller? *Ann Thorac Surg.* 2001;71:956-61.
- Yoshikawa K, Tsubota N, Kodama K, Ayabe H, Taki T, Mori T. Prospective study of extended segmentectomy for small lung tumors: the final report. *Ann Thorac Surg.* 2002;73:1055-9.
- Okada M, Koike T, Higashiyama M, Yamato Y, Kodama K, Tsubota N. Radical sublobar resection for small-sized non-small cell lung cancer: a multicenter study. *J Thorac Cardiovasc Surg.* 2006;132:769-75.
- Okada M, Tsutani Y, Ikeda T, Misumi K, Matsumoto K, Yoshimura M, et al. Radical hybrid video-assisted thoracic segmentectomy: long-term results of minimally invasive anatomical sublobar resection for treating lung cancer. *Interact Cardiovasc Thorac Surg.* 2012;14:5-11.
- Tsutani Y, Miyata Y, Nakayama H, Okumura S, Adachi S, Yoshimura M, et al. Prognostic significance of using solid versus whole tumor size on high-resolution computed tomography for predicting the pathological malignant grade of tumors in clinical stage IA lung adenocarcinoma: a multicenter study. *J Thorac Cardiovasc Surg.* 2012;143:607-12.
- Tsutani Y, Miyata Y, Nakayama H, Okumura S, Adachi S, Yoshimura M, et al. Prediction of pathological node-negative clinical stage IA lung adenocarcinoma for optimal candidates undergoing sublobar resection. *J Thorac Cardiovasc Surg.* 2012;144:1365-71.
- Goldstraw P, Crowley J, Chansky K, Giroux DJ, Groome PA, Rami-Porta R, et al. International Association for the Study of Lung Cancer International Staging Committee; Participating Institutions. The IASLC Lung Cancer Staging Project:

TABLE 5. Propensity score-matched comparison of clinical and pathologic factors between patients who underwent lobectomy and segmentectomy

	Lobectomy (n = 81)	Segmentectomy (n = 81)	P value
Clinical factors			
Age	66 (48-82)	65 (34-86)	.68
Gender			.74
Male	37 (45.6%)	34 (42.0%)	
Whole tumor size (cm)	2.0 (1.0-3.0)	1.7 (0.6-3.0)	.11
Solid tumor size (cm)	0.7 (0-2.0)	0.8 (0-3.0)	.17
SUVmax	1.4 (0-7.0)	1.2 (0-9.8)	.23
Side			.63
Right	33 (40.7%)	37 (45.6%)	
Lobe			.23
Upper	51 (63.0%)	43 (53.1%)	
Lower	30 (37.0%)	38 (46.9%)	
Pathologic factors			
Lymphatic invasion	10 (12.3%)	6 (7.4%)	.42
Vascular invasion	6 (7.4%)	6 (7.4%)	1.0
Pleural invasion	7 (8.6%)	4 (4.9%)	.45
Lymph node metastasis	3 (3.7%)	1 (1.2%)	.63

SUVmax, Maximum standardized uptake value.

- proposals for the revision of the TNM stage groupings in the forthcoming (seventh) edition of the TNM Classification of Malignant Tumours. *J Thorac Oncol.* 2007;2:706-14.
11. Delbeke D, Coleman RE, Guiberteau MJ, Brown ML, Royal HD, Siegel BA, et al. Procedure guideline for tumor imaging with 18F-FDG PET/CT 1.0. *J Nucl Med.* 2006;47:885-95.
 12. Mawlawi O, Podoloff DA, Kohlmyer S, Williams JJ, Stearns CW, Culp RF, et al. Performance characteristics of a newly developed PET/CT scanner using NEMA standards in 2D and 3D modes. *J Nucl Med.* 2004;45:1734-42.
 13. Nakayama H, Okumura S, Daisaki H, Kato Y, Uehara H, Adachi S, et al. Value of integrated positron emission tomography revised using a phantom study to evaluate malignancy grade of lung adenocarcinoma. *Cancer.* 2010;116:3170-7.
 14. Okada M, Nakayama H, Okumura S, Daisaki H, Adachi S, Yoshimura M, et al. Multicenter analysis of high-resolution computed tomography and positron emission tomography/computed tomography findings to choose therapeutic strategies for clinical stage IA lung adenocarcinoma. *J Thorac Cardiovasc Surg.* 2011;141:1384-91.
 15. Okada M, Tauchi S, Iwanaga K, Mimura T, Kitamura Y, Watanabe H, et al. Associations among bronchioloalveolar carcinoma components, positron emission tomographic and computed tomographic findings, and malignant behavior in small lung adenocarcinomas. *J Thorac Cardiovasc Surg.* 2007;133:1448-54.
 16. Tsutani Y, Miyata Y, Misumi K, Ikeda T, Mimura T, Hihara J, et al. Difference in prognostic significance of maximum standardized uptake value on [18F]-fluoro-2-deoxyglucose positron emission tomography between adenocarcinoma and squamous cell carcinoma of the lung. *Jpn J Clin Oncol.* 2011;41:890-6.
 17. Tsutani Y, Miyata Y, Yamanaka T, Nakayama H, Okumura S, Adachi S, et al. Solid tumors versus mixed tumors with a ground-glass opacity component in patients with clinical stage IA lung adenocarcinoma: prognostic comparison using high-resolution computed tomography findings. *J Thorac Cardiovasc Surg.* 2013;146:17-23.
 18. Nakamura K, Saji H, Nakajima R, Okada M, Asamura H, Shibata T, et al. A phase III randomized trial of lobectomy versus limited resection for small-sized peripheral non-small cell lung cancer (JCOG0802/WJOG4607L). *Jpn J Clin Oncol.* 2010;40:271-4.
 19. Keenan RJ, Landreneau RJ, Maley RH, Singh D, Macherey R, Bartley S, et al. Segmental resection spares pulmonary function in patients with stage I lung cancer. *Ann Thorac Surg.* 2004;78:228-33.
 20. Harada H, Okada M, Sakamoto T, Matsuoka H, Tsubota N. Functional advantage after radical segmentectomy versus lobectomy for lung cancer. *Ann Thorac Surg.* 2005;80:2041-5.

Methotrexate and gemcitabine combination chemotherapy for the treatment of malignant pleural mesothelioma

KOZO KURIBAYASHI^{1*}, SHIGERU MIYATA^{1*}, KAZUYA FUKUOKA¹, AKI MURAKAMI¹, SYUSAI YAMADA¹, KUNIHIRO TAMURA¹, NORIKO HIRAYAMA¹, TAKAYUKI TERADA¹, CHIHARU TABATA¹, YOSHIHIRO FUJIMORI² and TAKASHI NAKANO^{1,2}

¹Division of Respiratory Medicine, Department of Internal Medicine;
²Cancer Center, Hyogo College of Medicine, Nishinomiya, Hyogo 663-8501, Japan

Received December 15, 2012; Accepted April 9, 2013

DOI: 10.3892/mco.2013.118

Abstract. Malignant pleural mesothelioma (MPM) is an aggressive tumor of serosal surfaces with a poor prognosis. Methotrexate and gemcitabine have exhibited single-agent activity in MPM. We evaluated the feasibility of sequential administration of these agents in the treatment of MPM. A total of 21 patients with MPM received a 30-min infusion of 100 mg/m² methotrexate and, 30 min later, a 30-min infusion of 800 mg/m² gemcitabine. Twenty-four hours following the administration of methotrexate, leucovorin rescue therapy was initiated (10 mg/m² leucovorin administered 4 times at 6-h intervals). These treatments were administered weekly, with 4 weekly administrations constituting a cycle of therapy. A total of 88 cycles were administered to the 21 patients, with each patient receiving 1-10 cycles (median, 4.2 cycles). Eight patients (38.1%) exhibited a partial response, 10 patients (47.6%) had stable disease and 3 patients (14.3%) had progressive disease. The median overall survival was 19.4 months (range, 02-41 months). One-year and 2-year survival rates were 61.9 and 38.1%, respectively. Hematological toxicity was considered acceptable, with grade 3-4 toxicities occurring in 3 (14.3%) patients. Non-hematologic toxicity was generally mild. There was no treatment-related mortality. Our results suggest that methotrexate and gemcitabine combination therapy is feasible and effective in the treatment of MPM. This regimen may offer an alternative to platinum-based chemotherapy and a prospective trial including a larger cohort of patients is recommended to confirm these results.

Introduction

Malignant pleural mesothelioma (MPM) arises from the mesothelial surface of the pleural cavity and is a locally invasive tumor with poor prognosis (1,2). In >70% of patients, the tumor is associated with exposure to asbestos fibers following a long latent period of 20-50 years (3). The incidence of mesothelioma is rare in the general population; however, it is expected to increase in the next 20 years in industrialized countries as a result of past asbestos use (4,5).

MPM is refractory to the currently available treatment options. The efficacy of surgical therapy has not been precisely defined (6) and radiotherapy may be palliative but does not prolong survival (7). For the majority of patients with MPM, systemic chemotherapy remains the standard of care (8). Prior to 2003, the majority of studies on chemotherapy for MPM were conducted using either single agents or combination regimens in the setting of small phase II trials. The results demonstrated <20% of tumor regression with no significant effect on patient survival, which was 6-9 months (8,9). Since 2003, the combination of cisplatin and pemetrexed (PTX) has been used as standard chemotherapy for MPM (10). This was based on a randomized phase III study in which PTX plus cisplatin achieved a response rate of 41.3% and a median survival of 12.1 months, compared to 16.7% response rate and 9.3-month median survival achieved by cisplatin alone (10).

In this study, a non-platinum-based combination therapy with two anti-metabolites (methotrexate and gemcitabine) was devised. Methotrexate is an analogue of folic acid known to be effective against breast cancer, lymphoblastic leukemia and osteosarcoma (11,12). Gemcitabine is a pyrimidine analogue, effective against a wide range of solid tumors, including pancreatic carcinoma and non-small cell lung carcinoma (13). Methotrexate and gemcitabine have been reported to exhibit single-agent activity in MPM (8,9); however, the combined administration of these agents has not yet been investigated.

In the present study, we evaluated the feasibility and efficacy of methotrexate and gemcitabine combination therapy in the treatment of MPM, through the analysis of toxicity, response and survival data.

Correspondence to: Dr Yoshihiro Fujimori, Cancer Center, Hyogo College of Medicine, 1-1 Mukogawa-cho, Nishinomiya, Hyogo 663-8501, Japan
E-mail: fuji-y@hyo-med.ac.jp

*Contributed equally

Key words: malignant mesothelioma, chemotherapy, methotrexate, gemcitabine

Patients and methods

Patients. Patients with histologically confirmed MPM who had previously received 0-1 chemotherapy cycles, not including gemcitabine and methotrexate, were considered eligible for this single-center study. Tumor extension was classified according to the tumor-node-metastasis (TNM) staging system developed by the International Mesothelioma Interest Group (IMIG) (14). Patients were 18-75 years of age, with an Eastern Cooperative Oncology Group (ECOG) performance status of 0-2, had adequate bone marrow function (hemoglobin concentration ≥ 10 g/dl, total leukocyte count $\geq 3.0 \times 10^9/l$, granulocyte count $\geq 1.5 \times 10^9/l$ and platelet count $\geq 100 \times 10^9/l$), adequate renal function (serum creatinine level < 1.5 mg/dl) and adequate hepatic function (total bilirubin level ≤ 1.5 times the upper limit of normal and serum alanine transferase and alkaline phosphatase levels ≤ 3 times the upper limit of normal). Patients with a concurrent malignancy of another type or symptoms and/or signs of metastases in the central nervous system were excluded. Patients with prior surgery were considered eligible. This study was approved by the Institutional Review Board of Hyogo College of Medicine and informed consent was obtained from each patient.

Treatment. Patients received a 30-min intravenous (i.v.) infusion of 100 mg/m² methotrexate and, 30 min later, a 30-min i.v. infusion of 800 mg/m² gemcitabine. For leucovorin rescue, calcium leucovorin (10 mg/m², p.o. or i.v.) was administered 4 times at 6-h intervals, initiated 24 h after the administration of methotrexate. These treatments were administered weekly, with 4 treatments constituting a cycle of therapy. A maximum of 6 cycles were administered, unless therapy was terminated due to tumor progression, patient death or wish of treatment discontinuation, or in the presence of convincing evidence that further treatment was not beneficial. Antiemetic and symptomatic treatments were permitted. Analyses of blood cell count and chemistry were performed weekly. Treatment was delayed in the case of i) absolute neutrophil count $< 1.5 \times 10^9/l$ and/or platelet count $< 100 \times 10^9/l$; ii) any grade 3 or 4 non-hematological toxicity (except for nausea/vomiting) that did not resolve to grade 1 or less. If these toxicities were not resolved within the cycle, the dose was reduced to 75% of the previous dose level for the next cycle.

Response and toxicity criteria. Chest imaging by computed tomography (CT) was performed at baseline, following completion of every other treatment cycle and every 8 weeks following completion of therapy. Objective response was evaluated and calculated using the modified Response Evaluation Criteria in Solid Tumors (RESIST) criteria for MPM (15). Treatment-related toxicities were evaluated according to the National Cancer Institute Common Toxicity Criteria version 3.0 (16).

Statistical analysis. Survival was calculated as the time period from treatment initiation to death, using the Kaplan-Meier method (17).

Results

Patient characteristics. The characteristics of the 21 eligible patients are listed in Table I. There were 16 males and 5 females,

Table I. Patient characteristics.

Characteristics	No. (%)
Gender	
Male	16 (76.2)
Female	5 (23.8)
Age, years	
Median	63
Range	51-75
Performance status	
0	1 (4.8)
1	12 (57.1)
2	8 (38.1)
IMIG stage	
Ib	1 (4.8)
II	1 (4.8)
III	4 (19.0)
IV	15 (71.4)
Histological subtype	
Epithelial	17 (81.0)
Sarcomatous	3 (14.3)
Biphasic	1 (4.7)
Previous treatment	
None	10 (47.6)
Surgery	2 (9.5)
Chemotherapy	9 (42.9)
Asbestos exposure	
Yes	13 (61.9)
No	8 (38.1)

IMIG, International Mesothelioma Interest Group.

with a median age of 63 years (range, 51-75 years). The histological pattern of MPM was epithelial in 17 cases, sarcomatous in 3 cases and biphasic in 1 case. Nineteen patients (90.4%) had stage III and IV disease according to the IMIG staging system at the time of enrollment. Thirteen patients (61.9%) had an ECOG performance status of 0 or 1.

Responses to treatment. A total of 88 cycles were administered to the 21 patients. Each patient received a median 4.2 cycles (range, 2-10 cycles). Response to chemotherapy is shown in Table II. No patients exhibited a complete response. Eight patients (38.1%) exhibited a partial response. According to the histological pattern, a PR was observed in 6 out of the 17 patients with epithelial type and in 2 out of the 3 patients with sarcomatous type MPM. Out of the total 21 patients, 10 (47.6%) had stable disease and 3 (14.3%) had progressive disease with no period of stabilization.

Toxicity. The toxicity observed in each patient is shown in Table III. There was no treatment-related mortality. The most frequently observed hematological side effects were neutropenia and thrombocytopenia. Grade 3-4 hematologic

Table II. Response to chemotherapy and histologic subtype.

Response	Overall no. (%)	Histologic subtype		
		Epithelial no. (n)	Sarcomatous no. (n)	Biphasic no. (n)
Complete response	0	0	0	0
Partial response	8 (38.1)	6	2	0
Stable disease	10 (47.6)	8	1	1
Progressive disease	3 (14.3)	3	0	0

Table III. Chemotherapy-related toxicity in eligible patients.

Toxicity	Grade 1 no. (%)	Grade 2 no. (%)	Grade 3 no. (%)	Grade 4 no. (%)
Hematologic	5	2 (9.5)	2 (9.5)	1 (4.8)
Gastrointestinal	5 (23.8)	1 (4.8)	0 (0)	0 (0)
Hepatobiliary	4 (19.0)	3 (14.3)	0 (0)	0 (0)
Pulmonary	0 (0)	2 (9.5)	0 (0)	0 (0)

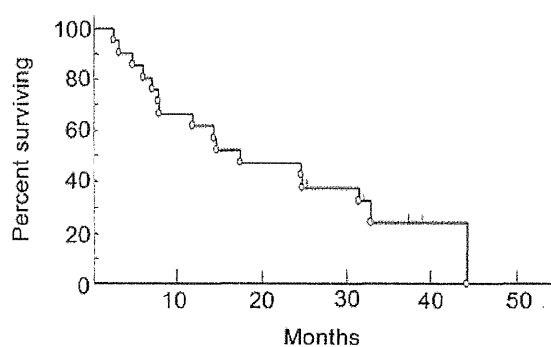


Figure 1. Overall survival.

toxicities were observed in 3 patients (14.3%), which, however, were manageable and did not result in life-threatening complications. Six patients (28.6%) experienced grade 1-2 gastrointestinal toxicities (nausea, vomiting and anorexia) and 7 patients (33.3%) developed grade 1-2 liver dysfunction. Two patients developed interstitial pneumonitis (grade 2) and were administered glucocorticosteroid therapy.

Survival. The median overall survival was 19.4 months (range, 2-41 months), with a 1- and 2-year survival rates of 61.9 and 38.1%, respectively (Fig. 1). As regards the histological pattern, the median survival was 19.6 months for the epithelial, 22.6 months for the sarcomatous and 7.1 months for the biphasic type of MPM.

Discussion

MPM is notoriously refractory to the majority of treatments and the standard first-line treatment is currently cisplatin and PTX chemotherapy (10). In the present study, we evaluated the

feasibility of a non-platinum regimen for MPM, involving the sequential administration of the anti-metabolites, methotrexate and gemcitabine.

Methotrexate, an antifolate, has long been used as an anticancer agent and exerts its action through the inhibition of dihydrofolate reductase (DHFR) (12). High-dose methotrexate (1500 mg/m²) has been reported to be effective in the treatment of MPM, with a response rate of 37% (18). However, high-dose methotrexate was associated with severe toxicity and this method of treatment has been abandoned. The efficacy of low- or medium-dose methotrexate has not been assessed in MPM. In the treatment of gastric cancer (19) and head and neck cancer (20), weekly administration of medium-dose methotrexate (100-200 mg/m²) combined with sequential administration of 5-fluorouracil (5-FU) (600 mg/m²) has been reported to be effective and of low toxicity. In this study, a moderate dose of methotrexate (100 mg/m²) was administered weekly in combination with gemcitabine.

PTX is a newly developed antifolate that targets multiple enzymes involved in DNA synthesis and folate metabolism. Single use of PTX has been reported to be moderately effective against MPM (21). Following combination therapy with 1,250 mg/m² gemcitabine administered on days 1 and 8 and 500 mg/m² PTX administered on day 8 or 1, chemotherapy-naïve MPM patients exhibited a response rate of 17-26%, with a median survival of 8-10 months (22). Hematologic toxicities included grade 3-4 neutropenia (60%) and febrile neutropenia (10%). These results indicated that the combination of PTX and gemcitabine was moderately effective in MPM patients but was associated with a notably high incidence of neutropenia (22).

In this study on the methotrexate and gemcitabine doublet regimen, 3 patients (14.3%) exhibited grade 3-4 hematologic toxicity, with no sepsis or hemorrhage. There was no observed grade 3-4 non-hematological toxicity. Two patients developed interstitial pneumonitis (grade 2) which responded well to

steroid therapy. Thus, the tolerability and toxicity profiles were considered acceptable.

The response rate with the methotrexate and gemcitabine combination chemotherapy was 38.1%, which is within the range of 20-50% observed with other 'active' agents for MPM (8,10). Median survival was 19.4 months. Antifolates may be one of the key agents for MPM, since the majority of mesothelioma cells of all histological MPM subtypes express high-affinity α folate receptor (23). In our combination regimen, we observed that methotrexate, an old-type antifolate, exhibited desirable efficacy. Methotrexate has also been reported to be more efficient compared to PTX, a newly developed antifolate, against osteosarcoma cells (24), indicating that methotrexate possesses a therapeutic potential.

In the present study, 10 out of the 21 patients were chemotherapy-naïve and their response rate to this regimen was similar to the overall response rate described above. This suggests that methotrexate plus gemcitabine may be beneficial as the first-line treatment for MPM. Eleven patients who had been previously treated also exhibited a response rate similar to the overall response rate. Although the optimal regimen constituting the second-line chemotherapy remains to be determined, results of the present study suggest that methotrexate plus gemcitabine may also be beneficial as a second-line treatment.

In conclusion, the present study demonstrated that the methotrexate and gemcitabine combination therapy is feasible, with a more favorable toxicity profile and efficient in the treatment of MPM. Further clinical evaluation is required, with prospective trials including a larger cohort of patients.

References

- Robinson BW, Musk AW and Lake RA: Malignant mesothelioma. *Lancet* 366: 397-408, 2005.
- Nakano T: Current therapies for malignant pleural mesothelioma. *Environ Health Prev Med* 13: 75-83, 2008.
- Wagner JC, Slegg CA and Marchand P: Diffuse pleural mesothelioma and asbestos exposure in North western Cape Province. *Br J Ind Med* 17: 260-271, 1960.
- Kaufman AJ and Pass HI: Current concepts in malignant pleural mesothelioma. *Expert Rev Anticancer Ther* 8: 293-303, 2008.
- Yang H, Testa JR and Carbone M: Mesothelioma epidemiology, carcinogenesis, and pathogenesis. *Curr Treat Options Oncol* 9: 147-57, 2008.
- Maziak DE, Gagliardi A, Haynes AE, Mackay JA and Evans WK: Surgical management of malignant pleural mesothelioma: a systematic review and evidence summary. *Lung Cancer* 48: 157-169, 2005.
- Ung YC, Yu E, Falkson C, Haynes AE, Stys-Norman D and Evans WK: The role of radiation therapy in malignant pleural mesothelioma: a systematic review. *Radiother Oncol* 80: 13-18, 2006.
- Steele JPC and Klabatsa A: Chemotherapy options and new advances in malignant pleural mesothelioma. *Ann Oncol* 16: 345-351, 2005.
- Fennell DA, Gaudino G, O'Byrne KJ, Mutti L and van Meerbeek J: Advances in the systemic therapy of malignant pleural mesothelioma. *Nat Clin Pract Oncol* 5: 136-147, 2008.
- Vogelzang NJ, Rusthoven JJ, Symanowski J, *et al*: Phase III study of pemetrexed in combination with cisplatin versus cisplatin alone in patients with malignant pleural mesothelioma. *J Clin Oncol* 21: 2636-2644, 2003.
- Huennkens FM: The methotrexate story: a paradigm for development of cancer chemotherapeutic agents. *Adv Enzyme Regul* 34: 397-419, 1994.
- McGuire JJ: Anticancer antifolates: current status and future directions. *Curr Pharm Des* 9: 2593-2613, 2003.
- Lund B, Kristjansen P and Hansen H: Clinical and preclinical activity of 2',2'-difluorodesoxycytidine (Gemcitabine). *Cancer Treat Rev* 19: 45-55, 1993.
- Rusch VW: A proposed new international TNM staging system for malignant pleural mesothelioma. From the International Mesothelioma Interest Group. *Chest* 108: 1122-1128, 1995.
- Byrne MJ and Nowak AK: Modified RECIST criteria for assessment of response in malignant pleural mesothelioma. *Ann Oncol* 15: 257-60, 2004.
- National Cancer Institute Common Toxicity Criteria for Adverse Events version 3.0. <http://ctep.cancer.gov/reporting/ctc.html>: Accessed August 9, 2003.
- Kaplan M and Meier P: Nonparametric estimation from incomplete observations. *J Am Stat Assoc* 53: 457-481, 1958.
- Solheim OP, Saeter G, Finnanger AM and Stenwig AE: High-dose methotrexate in the treatment of malignant mesothelioma of the pleura: a phase II study. *Br J Cancer* 65: 956-960, 1992.
- Imazawa M, Kojima T, Boku N, *et al*: Efficacy of sequential methotrexate and 5-fluorouracil (MTX/5FU) in improving oral intake in patients with advanced gastric cancer with severe peritoneal dissemination. *Gastric Cancer* 12: 153-157, 2009.
- Ringborg U, Ewert G, Kinnman J, Lundquist PG and Strander H: Methotrexate and 5-fluorouracil in head and neck cancer. *Semin Oncol* 10 (Suppl 2): 20-22, 1983.
- Scagliotti GV, Shin DM, Kindler HL, *et al*: Phase II study of pemetrexed with and without folic acid and vitamin B12 as front-line therapy in malignant pleural mesothelioma. *J Clin Oncol* 21: 1556-1561, 2003.
- Jänne PA, Simon GR, Langer CJ, *et al*: Phase II trial of pemetrexed and gemcitabine in chemotherapy-naïve malignant pleural mesothelioma. *J Clin Oncol* 26: 1465-1471, 2008.
- Bueno R, Appasani K, Mercer H, Lester S and Sugarbaker D: The alpha folate receptor is highly activated in malignant pleural mesothelioma. *J Thorac Cardiovasc Surg* 121: 225-233, 2001.
- Bodmer N, Walters DK and Fuchs B: Pemetrexed, a multitargeted antifolate drug, demonstrates lower efficacy in comparison to methotrexate against osteosarcoma cell lines. *Pediatr Blood Cancer* 50: 905-908, 2008.